catechols and inhibitor phenols generally enter the active site as the neutral species, but coordination to the metal center involves the corresponding anion.[21] Some basic species is therefore required to deprotonate the substrate/inhibitor, but the crystal structure indicates the absence of such species save for the coordinated ligands.[3] The coordinated hydroxide easily serves this function.

Last, we comment on the transformation of Fe(salps)Br to $Fe(HBT)_2Br$. This conversion entails an overall two-electron oxidation, consisting of the reductive cleavage of the S-S bond and the oxidative formation of two thiazole rings. While we have no insight into the mechanism of this reaction, it has been demonstrated that there is a tautomeric relationship between 2-(benzylideneamino)thiophenols and 2-arylbenzothiazolines, the latter yielding benzothiazoles upon two-electron oxidation.[9] The reaction we observe is presumably a metal-catalyzed autoxidation.

Acknowledgment. This work was supported by the National Institutes of Health (GM-33162).

Supplementary Material Available: Tables of positional and isotropic thermal parameters, anisotropic thermal factors, and bond angles for $[Fe(HBT)_2Br]\cdot 0.5C_7H_8$ (6 pages); a table of structure factors (6 pages). Ordering information is given on any current masthead page.

(21) May, S. W.; Phillips, R. S. *Biochemistry* **1979**, *18*, 5933-5939.

Contribution from the Lehrstuhl für Anorganische Chemie I, Ruhr-Universität, D-4630 Bochum, FRG, and Anorganisch-Chemisches Institut, Universität Heidelberg, D-6900 Heidelberg, FRG

Coordination Chemistry of Rhenium(V), -(IV), and -(III) with the Macrocyclic Ligands 1,4,7-Triazacyclononane (L) and Its N-Methylated Derivative (L'). Crystal Structures of $[LReCl_3]Cl$, $[L_2Re_2Cl_2(\mu\text{-}Cl)(\mu\text{-}OH)]I_2\cdot 2H_2O$, $[L_2Re_2I_2(\mu\text{-}O)_2]I_2\cdot 2H_2O$, and $[L'_2Re_2Cl_4(\mu\text{-}O)]ZnCl_4$. Effect of π-Donors on the Re-Re Bond Distance

Georg Böhm,[1a] Karl Wieghardt,*[,1a] Bernhard Nuber,[1b] and Johannes Weiss[1b]

Received January 29, 1991

The coordination chemistry of rhenium(III), -(IV), and -(V) with the macrocyclic triamines 1,4,7-triazacyclononane (L, $C_6H_{15}N_3$) and 1,4,7-trimethyl-1,4,7-triazacyclononane (L', $C_9H_{21}N_3$) has been investigated. Reaction of $[Re^{V}OCl_3(PPh_3)_2]$ with L and ethylene glycol in dry tetrahydrofuran affords monomeric $[LRe^{V}O(O_2C_2H_4)]^+$, which has been isolated in 75% yields as the bromide monohydrate (**1**) or the iodide monohydrate salt. The corresponding reaction with 1,2-dihydroxybenzene and 2-hydroxybenzyl alcohol gives $[LReO(O_2C_6H_4)]Br\cdot H_2O$ (**2**) and $[LReO(O_2C_7H_6)]I$ (**3**), respectively. **1** decomposes at 144 °C cleanly to give quantitatively ethylene and $[LRe^{VII}O_3]I$; **2** and **3** are stable up to 200 °C. **1** was found to be a useful starting material for the synthesis of mononuclear and dinuclear rhenium complexes containing the LRe fragment. Thus reduction of **1** in 1.0 M HCl or HBr with zinc affords $LRe^{III}X_3$ (X = Cl (**5**), Br (**6**)) both of which are oxidized in concentrated CH_3SO_3H in the presence of air to yield $[LRe^{IV}X_3]CH_3SO_3$ (X = Cl (**7**), Br (**8**)). **1** undergoes a series of disproportionation reactions in concentrated hydrohalide solutions. In refluxing 1.0 M HCl, *anti*-$[L_2Re^{IV}_2Cl_2(\mu\text{-}O)_2]I_2\cdot 2H_2O$ (**10**), $[L_2Re^{III}_2Cl_2(\mu\text{-}OH)(\mu\text{-}Cl)]I_2\cdot 2H_2O$ (**15**), and $[LReO_3]I$ are formed. From HBr and HI solutions of **1**, solid brown materials—presumably $[L_2Re^{IV}_2(OH)(H_2O)(\mu\text{-}O)_2]X_3$ (X = Br, I)—were isolated which formed upon heating to 120 °C $[L_2Re^{IV}_2X_2(\mu\text{-}O)_2]^{2+}$ (X = Br (**11**), I (**12**)). Oxidation of these brown solids in alkaline aqueous solution with air gives *anti*-$[L_2Re^{V}_2O_2(\mu\text{-}O)_2]^{2+}$ (**13**). From an aqueous solution of **13** the neutral complex $[L_2Re_2(OZnCl_3)_2(\mu\text{-}O)_2]$ (**14**) was isolated upon addition of $ZnCl_2$ and NaCl. Reduction of $[L'ReO_3]I$ with zinc affords the dinuclear complex $[L'_2Re_2Cl_4(\mu\text{-}O)]ZnCl_4$ (**9**). When the reduction is carried out in dry methanol $[L'ReO(OCH_3)_2]PF_6$ (**4**) is formed in ≈5% yield. Compounds **7**, **9**, **12**, and **15** have been characterized by X-ray crystallography. Crystal data: $[LReCl_3]Cl$ (**7**), space group *Pmnn* (No. 58), a = 7.842 (4) Å, b = 12.887 (7) Å, c = 12.998 (9) Å, V = 1313.58 Å^3, Z = 4; $[L'_2Re_2Cl_4(\mu\text{-}O)]ZnCl_4$ (**9**), space group *Pbnb* (No. 56), a = 8.614 (4) Å, b = 14.589 (8) Å, c = 25.24 (1) Å, V = 3181.84 Å^3, Z = 4; $[L_2Re_2I_2(\mu\text{-}O)_2]I_2\cdot 2H_2O$ (**12**), space group *Pmmn* (No. 58), a = 11.941 (5) Å, b = 8.410 (5) Å, c = 13.828 (6) Å, V = 1388.66 Å^3, Z = 2; $[L_2Re_2Cl_2(\mu\text{-}Cl)(\mu\text{-}OH)]I_2\cdot 2H_2O$ (**15**), space group $P\bar{1}$ (No. 2), a = 8.16 (1) Å, b = 8.41 (1) Å, c = 9.64 (1) Å, α = 84.4 (1)°, β = 81.3 (1)°, γ = 82.9 (1)°, V = 646.9 Å^3, Z = 1. The dinuclear complexes (edge sharing bioctahedra) **10**-**15** exhibit multiple metal-metal bonding with Re-Re distances ranging from 2.36 to 2.53 Å depending on the oxidation states of the rhenium centers and π-donor capacity of the terminal ligands. The new compounds have been characterized by UV-vis and NMR spectroscopy; their magnetic and electrochemical properties are also reported.

Introduction

Fusion of two octahedral transition-metal complexes via two μ-oxo bridges leading to an edge-sharing bis(μ-oxo)dimetal species is a very common structural motif in the coordination chemistry of early transition metals in high formal oxidation states.[2] If the metal ion has a d^0 electronic configuration and an oxidation state of +IV, +V or +VI, the metal-metal distance is governed by the $M-O_{oxo}$ bond distances and by a compromise between the electrostatic repulsion between the positively charged metal ions and the negatively charged O^{2-} ions of the bridges. This leads, in general, to metal-metal distances of 2.8-3.2 Å and obtuse M-O-M and acute O_{oxo}-M-O_{oxo} bond angles. Numerous complexes of this type have been crystallographically characterized. If, on the other hand, second- or third-row transition metals with a d^1, d^2, or d^3 electronic configuration are connected in this fashion, the metal-metal distances are usually much shorter (2.4-2.6 Å) and the M-O-M angles are acute whereas the O-M-O angles are obtuse. These structural features have been interpreted as a clear indication for direct metal-metal bonding in such dinuclear species.[3]

Previously, we have reported on the structural chemistry of a series of such complexes containing the dioxo-bis(μ-oxo)dimetal(V) core where the metal is molybdenum(V) and tungsten(V), respectively.[4] Structure A (depicted in Chart I) contains

(1) (a) Ruhr-Universität. (b) Universität Heidelberg.

(2) (a) *Comprehensive Coordination Chemistry*; Wilkinson, G., Gillard, R. D., McCleverty, J. A., Eds.; Pergamon Press: Oxford, England, 1987; Vols. III and IV. (b) Holm, R. H. *Chem. Rev.* **1987**, *87*, 1401. (c) Nugent, W. A.; Mayer, J. M. *Metal-Ligand Multiple Bonds*; Wiley: New York, 1988.

(3) (a) Cotton, F. A.; Ucko, D. A. *Inorg. Chim. Acta* **1972**, *6*, 161. (b) Shaik, S.; Hoffmann, R.; Fisel, C. R.; Summerville, R. H. *J. Am. Chem. Soc.* **1980**, *102*, 4555. (c) Cotton, F. A. *Polyhedron* **1987**, *6*, 667.

(4) (a) Wieghardt, K.; Hahn, M.; Swiridoff, W.; Weiss, J. *Angew. Chem., Int. Ed. Engl.* **1983**, *22*, 491. (b) Hahn, M.; Wieghardt, K. *Inorg. Chem.* **1984**, *23*, 3977. (c) Wieghardt, K.; Guttmann, M.; Chaudhuri, P.; Gebert, W.; Young, C.; Enemark, J. H. *Inorg. Chem.* **1985**, *24*, 3151. (d) Schreiber, P.; Wieghardt, K.; Flörke, U.; Haupt, H.-J. *Inorg. Chem.* **1988**, *27*, 2111.

0020-1669/91/1330-3464$02.50/0

Chart I

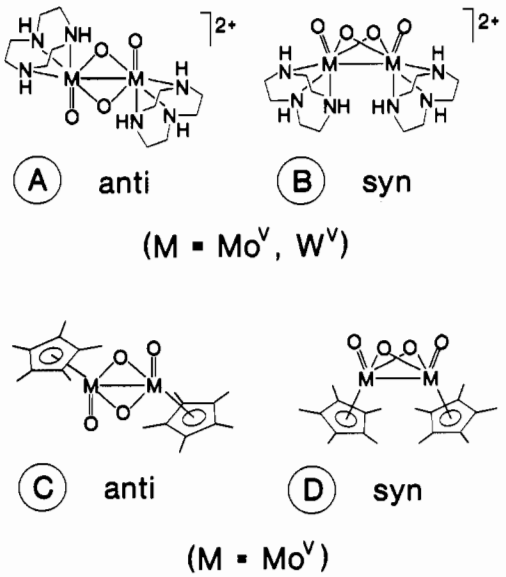

Chart II

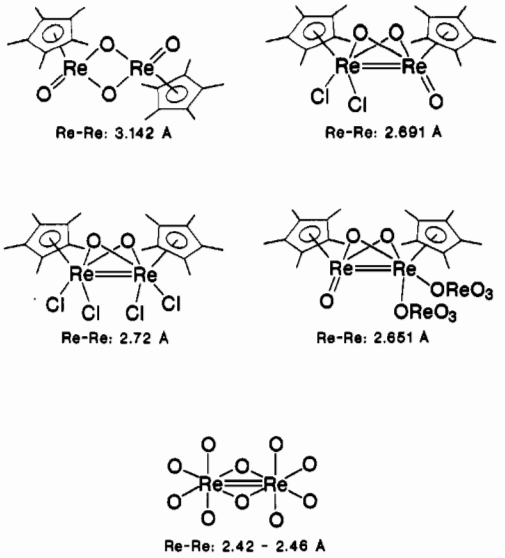

a terminal oxo ligand at each metal ion in the anti position with respect to each other and a planar four-membered $M_2(\mu\text{-}O)_2$ ring whereas in structure B the terminal oxo groups are syn with respect to each other and the $M_2(\mu\text{-}O)_2$ ring is puckered. The metal–metal distances in A and B are short and within experimental error identical (≈2.56 Å). Interestingly, the organometallic counterparts of A and B where the tridentate macrocycle 1,4,7-triazacyclononane (L) is replaced by a bound pentamethylcyclopentadienyl anion (Cp^{*-}), namely C and D, have also been characterized.[5] The structural features of the $O_2Mo_2(\mu\text{-}O)_2$ cores in C and D are very similar to those in A and B except that the metal–metal distances are slightly longer (C, 2.647 (3) Å; D, 2.587 (1) Å). The short metal–metal distances and the observed diamagnetism of the Mo^V and W^V (d^1) complexes are indicative of a metal–metal bond order 1.

Edge-sharing bioctahedral complexes may in principle exhibit M–M bond orders of 1–3, by overlap of pairs of metal d orbitals affording a σ, a π, and a δ bond.[3c] M=M double bonds in complexes with a bis(μ-oxo)dimetal core are quite rare.[6] Rhenium(V) possesses a d^2 electron configuration and is therefore an excellent candidate for the construction of such species, but only a few solid-state structures such as $Nd_4Re_2O_{11}$[7] and $La_6Re_4O_{18}$[8] have been structurally characterized that contain dimeric building blocks with a $Re^V_2(\mu\text{-}O)_2$ unit.[9] Short Re–Re bonds at 2.42–2.46 Å have been measured in accord with the above notion of double bonds between the Re^V ions. It is therefore unexpected that in the diamagnetic Re^V analogue of C, $[Cp_2{}^*Re_2O_2(\mu\text{-}O)_2]\cdot 2H_2O$, the Re–Re distance is 3.142 Å and the Re–O–Re angles are obtuse.[10] Clearly, no metal–metal bond is present in this compound (Chart II). Formal substitution of one or both terminal oxo ligands by two or four chloride ions in $Cp_2{}^*Re_2OCl_2(\mu\text{-}O)_2$ and $Cp_2{}^*Re_2Cl_4(\mu\text{-}O)_2$ yields Re–Re distances at 2.691 and 2.72 Å, respectively, indicating the presence of metal–metal bonding.[10] What are the electronic factors that govern this dichotomy?

We felt it worthwhile to synthesize the Werner-type Re^V analogue of A (or B), $[L_2Re_2O_2(\mu\text{-}O)_2]^{2+}$, and determine its structure in order to establish the presence or absence of a Re–Re bond. Furthermore, dinuclear bioctahedral complexes of Re^{IV} (d^3) with a $Re^{IV}_2(\mu\text{-}O)_2$ moiety would also be of great interest in this respect since a Re–Re triple bond might be expected. To our knowledge only one such species has previously been structurally characterized,[11] $K_4[Re^{IV}_2(C_2O_4)_4(\mu\text{-}O)_2]\cdot 3H_2O$, which contains a very short Re–Re bond at 2.362 (1) Å. Here we report the synthesis of three such $[L_2Re_2X_2(\mu\text{-}O)_2]^{2+}$ (X = Cl, Br, I) complexes. The structures of the chloro and iodo species have been determined by X-ray crystallography.

The synthesis of these binuclear complexes proved to be quite difficult. A readily accessible reactive mononuclear complex containing the LRe fragment was finally found by the reaction of $ReOCl_3(PPh_3)_2$, the tridentate ligand 1,4,7-triazacyclononane, and glycol in dry tetrahydrofuran. $[LReO(O_2C_2H_4)]^+$ is a useful starting material for the synthesis of other mononuclear and dinuclear rhenium complexes. The LRe fragment is thermodynamically stable and kinetically inert and allows metal-centered redox reactions and substitution reactions at the other coordination sites of the Re center without concomitant dissociation of the LRe fragment.[12] Some aspects of this work have been published in a preliminary communication.[13]

Experimental Section

The ligands 1,4,7-triazacyclononane (L) and 1,4,7-trimethyl-1,4,7-triazacyclononane (L′) and the complex $ReOCl_3(PPh_3)_2$ were prepared as described in the literature.[14,15] All other reagents and solvents were obtained from commercial sources.

Infrared spectra were recorded in the range 4000–400 cm^{-1} as KBr disks on a Perkin Elmer FT-IR spectrometer Model 1720 X. Infrared spectra in the range 400–200 cm^{-1} were recorded as CsI disks on a Bruker IF S-85 spectrometer. Electronic absorption spectra were recorded in the range 200–2000 nm on a Perkin-Elmer Lambda spectrophotometer. Cyclic voltammetric measurements were carried out by the use of PAR equipment (potentiostat Model 173, universal programmer Model 175) on acetonitrile solutions that contained 0.1 M tetra-*n*-butylammonium hexafluorophosphate ($[TBA]PF_6$) as the supporting electrolyte. $E_{1/2}$ values, determined as $(E_{p,a} + E_{p,c})/2$, were referenced to the Ag/AgCl electrode (LiCl, C_2H_5OH) at ambient temperature and are uncorrected for junction potentials. Under our experimental conditions, the ferrocenium/ferrocene couple is at $E_{1/2}$ = +0.51 V vs Ag/AgCl.

(5) (a) Arzoumanian, H.; Baldy, A.; Pierrot, M.; Petrignani, J.-F. *J. Organomet. Chem.* **1985**, *294*, 327. (b) de Jesus, E.; de Miguel, A. V.; Royo, P.; Manotti-Lanfredi, A. M.; Tiripicchio, A. *J. Chem. Soc., Dalton Trans.* **1990**, 2779.
(6) Cotton, F. A.; Walton, R. A. *Multiple Bonds between Metal Atoms*; Wiley: New York, 1982.
(7) Wilhelmi, K. A.; Lagervall, E.; Müller, O. *Acta Chem. Scand.* **1970**, *24*, 3406.
(8) Besse, J.-P.; Band, G.; Chevalier, R.; Gasparin, M. *Acta Crystallogr., Sect. B* **1978**, *34*, 3532.
(9) Perrin, A.; Sergent, M. *New J. Chem.* **1988**, *12*, 337.
(10) Herrmann, W. A.; Flöel, M.; Kulpe, J.; Felixberger, J. K.; Herdtweck, E. *J. Organomet. Chem.* **1988**, *355*, 297.
(11) Lis, T. *Acta Crystallogr., Sect. B* **1975**, *31*, 1594.
(12) Recent review articles on the coordination chemistry of tridentate macrocyclic amines: (a) Chaudhuri, P.; Wieghardt, K. *Prog. Inorg. Chem.* **1987**, *35*, 329. (b) Bhula, R.; Osvath, P.; Weatherburn, D. C. *Coord. Chem. Rev.* **1988**, *91*, 89.
(13) Böhm, G.; Wieghardt, K.; Nuber, B.; Weiss, J. *Angew. Chem., Int. Ed. Engl.* **1990**, *29*, 787.
(14) (a) Atkins, T. J.; Richman, J. E.; Oettle, W. F. *Org. Synth.* **1978**, *58*, 86. (b) Wieghardt, K.; Chaudhuri, P.; Nuber, B.; Weiss, J. *Inorg. Chem.* **1982**, *21*, 3086.
(15) Johnson, N. P.; Lock, C. J.; Wilkinson, G. *J. Chem. Soc.* **1964**, 1054.

Magnetic susceptibilities of powdered samples were measured by using the Faraday method in the temperature range 90–298 K. Corrections for diamagnetism were applied with use of Pascal's constants.

Syntheses of Complexes. Reactions carried out in "deoxygenated solutions" were run under a nitrogen-blanketing atmosphere. Where no specific atmosphere is designated, the reactions were carried out in air. Aqueous solutions of HCl or HBr were used throughout this study.

$[LReO(C_2H_4O_2)]Br\cdot H_2O$ (1). To a deoxygenated solution of 1,4,7-triazacyclononane (L) (0.52 g, 4.02 mmol) and freshly distilled ethylene glycol (0.19 g, 3.06 mmol) in dry tetrahydrofuran (THF) (60 mL) was added $[ReOCl_3(PPh_3)_2]$ (1.57 g, 1.88 mmol). The solution was stirred for 2 h at room temperature. A faint blue precipitate of $[LReO(O_2C_2H_4)]Cl$ formed, which was filtered off and dissolved in water (30 mL) and the resulting solution filtered. Addition of a saturated aqueous NaBr solution (10 mL) initiated the precipitation of blue crystals, which were filtered off and air-dried; yield 1.10 g (75%). The iodide salt $[LReO(O_2C_2H_4)]I\cdot H_2O$ was prepared analogously by using a saturated NaI solution. IR (KBr, cm^{-1}): ν(Re=O) = 961; ν(Re—OC) = 654, 615. ^1H NMR (D_2O): δ 2.5–3.8 (m, $-CH_2-$ of L), 4.3–4.7 (m, $-CH_2-$ of glycolate). Anal. Calcd for $C_8H_{21}N_3O_4BrRe$ (mol wt 489.38): C, 19.63; H, 4.33; N, 8.59; Br, 16.33. Found: C, 19.7; H, 4.4; N, 8.6; Br, 16.3.

$[LReO(O_2C_6H_4)]Br\cdot H_2O$ (2). To a deoxygenated solution of L (0.26 g, 2.01 mmol) and 1,2-dihydroxybenzene (0.17 g, 1.54 mmol) in dry THF (30 mL) was added $[ReOCl_3(PPh_3)_2]$ (0.84 g, 1.01 mmol). After the mixture was stirred for 2 h at 20 °C, a brown precipitate formed, which was filtered off and recrystallized from water (20 mL) and a saturated aqueous NaBr solution (5 mL); yield 0.29 g (53%). IR (KBr, cm^{-1}): ν(Re=O) = 964; ν(Re—OC) = 679, 667; ν(C—O) = 1242, 1225. ^1H NMR (D_2O): δ 2.5–3.8 (m, $-CH_2-$ of L), 6.7–7.1 (m, C_6H_4). ^{13}C NMR (dmso): δ 167.8, 121.3, 114.0 (aromatic C atoms), 62, 52, 44 ($-CH_2-$ of L). Anal. Calcd for $C_{12}H_{21}BrN_3O_4Re$ (mol wt 537.43): C, 26.82; H, 3.94; N, 7.82; Br, 14.87. Found: C, 27.1; H, 3.8; N, 8.0; Br, 15.0.

$[LReO(O_2C_7H_6)]I$ (3). To a deoxygenated solution of L (0.26 g, 2.01 mmol) and 2-hydroxybenzylalcohol (0.19 g, 1.53 mmol) in dry THF (30 mL) was added $[ReOCl_3(PPh_3)_2]$ (0.84 g, 1.01 mmol). The solution was stirred for 2 h at 20 °C. The green-brown precipitate was filtered off and recrystallized from water (20 mL) and a saturated aqueous NaI solution (5 mL). Bluish green crystals formed from such a solution within 2 days; yield 0.30 g (51%). IR (KBr, cm^{-1}): ν(Re=O) = 957; ν(Re—OC) = 632, 581. Anal. Calcd for $C_{13}H_{21}N_3O_3IRe$ (mol wt 580.44): C, 26.90; H, 3.65; N, 7.24. Found: C, 26.8; H, 3.6; N, 7.2.

$[L'ReO(OCH_3)_2]PF_6$ (4). A mixture of $[L'ReO_3]I$[16] (0.53 g, 1.0 mmol) and zinc powder (0.70 g) in dry methanol (30 mL) was heated to reflux for 2 h after which time the cooled (20 °C) solution was filtered. To the clear, light green solution was added $[TBA]PF_6$ (2.0 g) dissolved in methanol. Upon storage of this solution at 2 °C for 3 days, a few blue crystals of **4** precipitated, which were filtered off and air-dried; yield 0.03 g (5%). IR (KBr, cm^{-1}): ν(Re=O) = 947; ν(C—O) = 1021; ν(Re—OC) = 533. ^1H NMR (acetone-d_6; 80 MHz): δ 2.7–4.1 (m, $-CH_2-$, CH_3 of L'), 4.9 (s, OCH_3). Anal. Calcd for $C_{11}H_{27}N_3O_3RePF_6$ (mol wt 580.52): C, 22.76; H, 4.69; N, 7.24. Found: C, 22.5; H, 4.6; N, 7.1.

$LReX_3$ (X = Cl (5), Br (6)). To a reaction mixture of **1** (0.245 g, 0.50 mmol) in 1.0 M hydrochloric and hydrobromic acid (15 mL), respectively, at 40 °C was added zinc powder (0.30 g) in small amounts within 2 h. During this time an orange and red precipitate formed, respectively, which was filtered off, washed with H_2O and acetone, and air-dried. Yield: 0.13 g (62%) of **5**; 0.17 g (61%) of **6**. IR (CsI, cm^{-1}) of **5**: ν(Re–Cl) = 290, 310. Anal. Calcd for $C_6H_{15}N_3Cl_3Re$ (mol wt 421.76): C, 17.09; H, 3.58; N, 9.96; Cl, 25.2. Found: C, 16.8; H, 3.4; N, 9.5; Cl, 25.1. Anal. Calcd for $C_6H_{15}N_3Br_3Re$ (mol wt 555.13): C, 12.98; H, 2.72; N, 7.57; Br, 43.2. Found: C, 13.1; H, 2.6; N, 7.6; Br, 43.1.

$[LReCl_3](CH_3SO_3)$ (7) and $[LReBr_3](CH_3SO_3)\cdot H_2O$ (8). When a reaction mixture of 0.50 mmol of **5** and **6**, respectively, was heated to 100 °C in methanesulfonic acid (10 mL) in the presence of air, a color change to brown-green is observed within a few minutes. To the cooled solution (0 °C) was added diethyl ether dropwise with efficient cooling, which initiated the precipitation of light green microcrystalline **7** and **8**, respectively, in ≈50% yield. $[LReCl_3]Cl$ was obtained from a reaction mixture of **1** (0.27 g, 0.50 mmol) in 10 M HCl (15 mL) at 40 °C to which zinc powder (0.30 g) was added in small amounts. After 2 h, a clear green solution was obtained from which green crystals of $[LReCl_3]Cl$ precipitated in 22% yield. These crystals were found to be suitable for an X-ray structure determination. IR (CsI, cm^{-1}) of **7**: ν(Re–Cl) = 354, 337. IR (CsI, cm^{-1}) of **8**: ν(Re–Br) = 230. μ_{eff} of **7** = 3.6 μ_B (Θ = −13.2 K); μ_{eff} of **8** = 3.6 μ_B (Θ = −11.5 K). Anal. Calcd for $C_7H_{18}N_3Cl_3O_3SRe$ (mol wt 516.85): C, 16.27; H, 3.51; N, 8.13; Cl, 20.6. Found: C, 16.4; H, 3.4; N, 8.1; Cl, 20.5. Anal. Calcd for $C_7H_{20}N_3Br_3O_4SRe$ (mol wt 668.24): C, 12.58; H, 3.02; N, 6.29; Cl, 35.9. Found: C, 12.5; H, 3.0; N, 6.2; Cl, 35.6. Anal. Calcd for $C_6H_{15}N_3Cl_4Re$ (mol wt 457.21): C, 15.76; H, 3.31; N, 9.19; Cl, 31.0. Found: C, 15.6; H, 3.2; N, 9.4; Cl, 30.9.

$[L'_2Re_2Cl_4(\mu\text{-}O)][ZnCl_4]$ (9). To a solution of $[L'ReO_3]I$[16] (0.27 g, 0.51 mmol) in 0.5 M HCl (20 mL) was added zinc powder (0.33 g) in small amounts at 60 °C. The color of the solution changed from colorless to blue to green and, finally, to deep brown. After the mixture was cooled to 25 °C, a solution of $ZnCl_2$ (0.82 g, 6.02 mmol) dissolved in 0.5 M HCl (5 mL) was added. A brown precipitate formed within 1 h, which was filtered off and recrystallized from 0.5 M HCl; yield 0.20 g (36%). Anal. Calcd for $C_{18}H_{42}N_6Cl_8ORe_2Zn$ (mol wt 1080.00): C, 20.02; H, 3.92; N, 7.78; Cl, 26.26. Found: C, 19.9; H, 4.1; N, 7.6; Cl, 25.9.

The perchlorate salt $[L'_2Re_2Cl_4(\mu\text{-}O)](ClO_4)_2$ was prepared by dissolving crude **9** (0.20 g) in a water/dimethylformamide (1:1) mixture (20 mL) to which $NaClO_4$ (3.0 g) was added. The mixture was gently heated until a clear brown solution was obtained, which was allowed to stand in an open vessel for 10 days. Large, brown crystals precipitated out, which were filtered off and air-dried.

***anti*-$[L_2Re_2Cl_2(\mu\text{-}O)_2]I_2\cdot 2H_2O$ (10). Method A.** A solution of **1** (0.27 g, 0.50 mmol) in 0.5 M HCl (20 mL) was heated under reflux for 3 h. The solution was allowed to cool to 25 °C, and a concentrated aqueous NaI (1.5 g) solution (10 mL) was added. Within 2 days at 20 °C, black and colorless crystals of **10** and $[LReO_3]I$ precipitated from the deep brown solution. The black crystals were separated out manually under a microscope and recrystallized from 0.5 M HCl; yield 0.15 g (30%).

Method B. A reaction mixture of **5** (0.21 g, 0.50 mmol) in 1.0 M methanesulfonic acid (15 mL) was heated under reflux in the presence of air for 3 h. To the cooled (20 °C), deep brown solution was added NaI (1.5 g) dissolved in water (10 mL). From this solution, large black crystals precipitated out within 3 days, which were filtered off and air-dried; yield 0.30 g (59%). IR (KBr, cm^{-1}): ν(Re–O–Re) = 694. Anal. Calcd for $C_{12}H_{34}N_6O_4Cl_2I_2Re_2$ (mol wt 1023.57): C, 14.08; H, 3.35; N, 8.21; I, 24.80; Cl, 6.93. Found: C, 14.3; H, 3.4; N, 8.2; I, 25.0; Cl, 6.85.

***anti*-$[L_2Re_2Br_2(\mu\text{-}O)_2]Br_2\cdot 2H_2O$ (11).** A solution of the bromide salt of **1** (0.27 g, 0.55 mmol) in 0.5 M HBr (20 mL) was heated under reflux for 3 h. To the cooled (20 °C) solution was added a concentrated aqueous solution of NaBr (1.5 g). Within 2 days, black crystals and colorless crystals of $[LReO_3]Br$ precipitated out of the deep brown solution. The black crystals were separated out manually and heated to 120 °C for 12 h. The resulting material was dissolved in water. Slow evaporation of the solvent in an open vessel gave large, black crystals; yield 0.16 g (24%). IR (KBr, cm^{-1}): ν(Re–O–Re) = 706. Anal. Calcd for $C_{12}H_{34}N_6O_4Br_4Re_2$ (mol wt 1018.47): C, 14.15; H, 3.36; N, 8.25; Br, 31.38. Found: C, 14.1; H, 3.2; N, 8.3; Br, 31.6.

***anti*-$[L_2Re_2I_2(\mu\text{-}O)_2]I_2\cdot 2H_2O$ (12).** A solution of **1** (0.27 g, 0.50 mmol) in 0.5 M HI was heated under reflux for 3 h. After the mixture was cooled to 20 °C and a concentrated aqueous solution (10 mL) of NaI (1.5 g) was added, brown-black and colorless crystals precipitated out within 3 days. The brown-black crystals were separated out manually and heated to 120 °C for 12 h. The resulting material was recrystallized from a small amount of water. Slow evaporation of the solvent from the purple solution gave large, black crystals of **12**, which were suitable for an X-ray structure determination; yield 0.18 g (30%). IR (KBr, cm^{-1}): ν(Re–O–Re) = 702. Anal. Calcd for $C_{12}H_{34}N_6O_4I_4Re_2$ (mol wt 1206.47): C, 11.95; H, 2.84; N, 6.97; I, 42.07. Found: C, 11.7; H, 2.8; N, 6.8; I, 42.2.

"$[L_2Re_2(OH)(H_2O)(\mu\text{-}O)_2]I_3$". A solution of **1** (0.27 g, 0.50 mmol) in 0.5 M HI was heated under reflux for 3 h. After the solution was cooled to 20 °C, a saturated aqueous solution (10 mL) of NaI (1.5 g) added, and the mixture allowed to stand for 3 days, black crystals precipitated along with a minor colorless component ($[LReO_3]I$); yield 0.13 g (24%). This material analyzed as L:I = 2:3 and is tentatively formulated as $[L_2Re_2(OH)(H_2O)(\mu\text{-}O)_2]I_3$. Anal. Calcd for $C_{12}H_{33}N_6Re_2O_4I_3$: C, 13.36; H, 3.08; N, 7.79; I, 35.30. Found: C, 13.14; H, 3.11; N, 7.69; I, 35.14.

***anti*-$[L_2Re_2O_2(\mu\text{-}O)_2]I_2$ (13).** An aqueous solution (25 mL) of **1** (0.27 g, 0.50 mmol) was stirred over zinc amalgam (20%, 5 g) under an argon atmosphere at 40 °C for 3 h. The resulting green-brown solution was separated from the zinc amalgam and was stirred for 24 h at room temperature during which time the color changed to purple. After addition of a saturated aqueous solution of NaI (15 mL) purple microcrystals precipitated out, which were filtered off and air-dried; yield 0.28 g (60%). Recrystallization from a minimum amount of water (50 °C) produced purple crystals of X-ray quality. IR (KBr, cm^{-1}): ν(Re=O) = 818, 794; ν(Re—O—Re) = 729. Anal. Calcd for $C_{12}H_{30}N_6O_4I_2Re_2$ (mol wt 948.63): C, 15.19; H, 3.19; N, 8.86; I, 26.75. Found: C, 15.1; H, 3.1; N, 9.0; I, 26.4.

***anti*-$[L_2Re_2(OZnCl_3)_2(\mu\text{-}O)_2]$ (14).** To an aqueous solution (20 mL) of $ZnCl_2$ (0.82 g, 6.01 mmol) and NaCl (0.70 g, 12.0 mmol) was added a few drops of 0.1 M CH_3SO_3H until a clear solution was obtained to

(16) Pomp, C.; Wieghardt, K. *Polyhedron* **1988**, *7*, 2537.

Table I. Crystallographic Data of Complexes

	7	9	12	15
chem formula	$[(C_6H_{15}N_3)ReCl_3]Cl$	$[(C_9H_{21}N_3)_2Re_2Cl_4O]ZnCl_4$	$[(C_6H_{15}N_3)_2Re_2I_2O_2]I_2\cdot 2H_2O$	$[(C_6H_{15}N_3)_2Re_2Cl_3(OH)]I_2\cdot 2H_2O$
fw	457.22	1080.00	1206.47	1044.03
space group	*Pmnn* (No. 58)	*Pbnb* (No. 56)	*Pnmn* (No. 58)	$P\bar{1}$ (No. 2)
a, Å	7.842 (4)	8.614 (4)	11.941 (5)	8.16 (1)
b, Å	12.887 (7)	14.589 (8)	8.410 (5)	8.41 (1)
c, Å	12.998 (9)	25.24 (1)	13.828 (6)	9.64 (1)
α, deg				84.4 (1)
β, deg				81.3 (1)
γ, deg				82.9 (1)
V, Å^3	1313.58	3181.84	1388.66	646.9
Z	4	4	2	1
T, °C	22	22	22	22
radiation (λ, Å)	0.71073	0.71073	0.71073	0.71073
ρ_{calcd}, g cm^{-3}	2.31	2.25	2.88	2.68
μ(Mo Kα), cm^{-1}	101.7	91.7	132.6	121.8
transm coeff	0.30–1.00	0.615–1.00	0.33–1.00	0.25–1.00
R^a	0.040	0.042	0.039	0.060
R_w^b	0.036	0.039	0.037	0.051

$^a R = \sum||F_o| - |F_c||/\sum|F_o|$. $^b R_w = [\sum w(|F_o| - |F_c|)^2/\sum w|F_o|^2]^{1/2}$; $w = 1/\sigma_F^2$.

which **13** (0.47 g, 0.50 mmol) was added with stirring for 3 h at 30 °C. From the clear, green brownish solution, brown crystals suitable for X-ray crystallography separated out within 2 days, which were filtered off and air-dried; yield 0.21 g (40%). IR (KBr, cm^{-1}): $\nu_{as}(Re_2O_2)$ = 712; ν(Re–O–Zn) = 555, 535. Anal. Calcd for $C_{12}H_{30}N_6O_4Cl_6Re_2Zn_2$ (mol wt 1038.32): C, 13.88; H, 2.91; N, 8.09; Cl, 20.49. Found: C, 13.6; H, 3.1; N, 8.0; Cl, 20.5.

***anti*-[$L_2Re_2(\mu$-Cl)(μ-OH)]$I_2\cdot 2H_2O$ (15).** A solution of **1** (0.54 g, 1.00 mmol) in 1.0 M aqueous HCl (20 mL) was heated under reflux for 3 h. Addition of NaI (1.5 g) dissolved in 5 mL of water initiated the crystallization of **10** and $[LReO_3]I$ within 2 days at 20 °C. The solid material was filtered off, and the filtrate was stored at 2 °C in the refrigerator for a further 2 days. A deep blue precipitate formed, which was filtered off and air-dried. Recrystallization from 1 M HCl produced deep blue crystals of X-ray quality upon slow evaporation of the hydrochloric acid; yield 0.10 g (10%). Anal. Calcd for $C_{12}H_{35}N_6O_3Cl_3I_2Re_2$ (mol wt 1044.03): C, 13.81; H, 3.38; N, 8.05; I, 24.31; Cl, 10.19. Found: C, 14.1; H, 3.1; N, 8.0; I, 24.0; Cl, 9.9.

***anti*-[$L_2Re_2Br_2(\mu$-Br)(μ-OH)]$I_2\cdot 2H_2O$ (16).** Blue-black crystals of this complex were prepared as described above for **15** by using HBr instead of HCl; yield 0.12 g (11%). Anal. Calcd for $C_{12}H_{35}N_6O_3Br_3I_2Re_2$ (mol wt 1177.38): C, 12.24; H, 3.00; N, 7.14; I, 21.56. Found: C, 12.1; H, 3.1; N, 7.2; I, 21.2.

X-ray Crystallography. Crystal data, data collection, and refinement are summarized in Table I (and Table S1, supplementary material). A green crystal of **7**, black crystals of **9** and **12**, and a blue crystal of **15** were mounted on a glass fiber and placed on a Syntex R3 or AED II (Siemens) diffractometer. Graphite-monochromated Mo Kα X-radiation was used throughout. Unit cell parameters were determined in all cases by the automatic indexing of 35 centered reflections. Intensity data were corrected for Lorentz, polarization and absorption effects (empirical ψ scans of eight reflections in the range $6 \le 2\theta \le 50°$) in the usual manner. The structures were solved by conventional Patterson and difference Fourier methods by using the SHELXTL-PLUS program package.[17] The function minimized during full-matrix least-squares refinement was $\sum w(|F_o| - |F_c|)^2$ where $w = 1/\sigma^2(F)$. Neutral-atom scattering factors and an anomalous dispersion correction for non-hydrogen atoms were taken from ref 18. The positions of the hydrogen atoms of the methylene and methyl groups were placed at calculated positions with group isotropic thermal parameters while the methyl groups in **9** were treated as rigid bodies, each with three rotational variables. All non-hydrogen atoms were refined with anisotropic thermal parameters. The final difference Fourier syntheses showed residual electron density of ca. 1.2–2.0 e/Å^3 in the neighborhood of the heavy atom Re, which was considered to be chemically insignificant.

Results

Syntheses of Mononuclear Complexes. Scheme I summarizes the preparative routes to mononuclear rhenium complexes containing the macrocycle 1,4,7-triazacyclononane (L). Reaction of ethylene glycol, $[ReOCl_3(PPh_3)_2]$, and the ligand L in dry

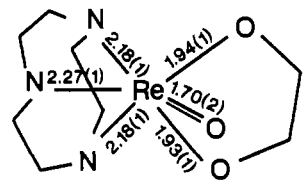

Figure 1. Structure of the cation in crystals of $[LReO(O_2C_2H_4)]Br\cdot H_2O$ (**1**) with selected bond distances (Å).[13]

Scheme I. Syntheses of Mononuclear Complexes

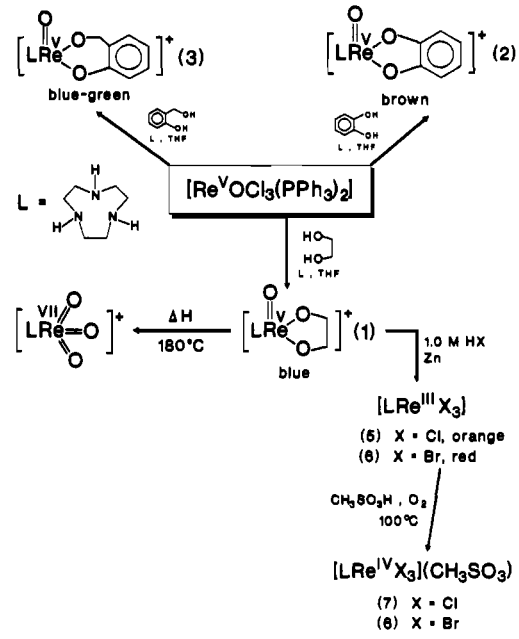

tetrahydrofuran (THF) at room temperature affords a pale blue microcrystalline precipitate of $[LReO(O_2C_2H_4)]Cl$ in ≈75% yield, which can be converted to the corresponding bromide monohydrate **1** or iodide monohydrate salts by recrystallization from water and addition of NaBr and NaI, respectively. The reaction proceeds most probably via the $[LReOCl_2]^+$ intermediate.[16] **1** is stable both in solution and in the solid state in the presence of air. $[LReO(O_2C_2H_4)]Br\cdot H_2O$ is diamagnetic (d^2) and has been characterized by X-ray crystallography.[13] Figure 1 shows the structure of the monocation and summarizes some important bond distances.

1,2-Dihydroxybenzene and 2-hydroxybenzyl alcohol react by using the same conditions as described for **1** to give the analogous diamagnetic complexes $[LReO(O_2C_6H_4)]^+$ and $[LReO(O_2C_7H_6)]^+$ which have been isolated as bromide monohydrate (**2**) and iodide salts, respectively. The analogous bis(methoxy)

(17) Full-matrix least-squares structure refinement program package SHELXTL-PLUS: Sheldrick, G. M., University of Göttingen.
(18) *International Tables of Crystallography*; Kynoch: Birmingham, England, 1974; Vol. IV, pp 99, 149.

Table II. Electronic Spectral Data[a] and Magnetic Properties of Complexes

complex	solvent	λ_{max}, nm (ϵ, L mol^{-1} cm^{-1})	magnetism
$[LReO(O_2C_2H_4)]Br\cdot H_2O$ (**1**)	H_2O	546 (29), 225 (4800)	diamagnetic
$[LReO(O_2C_6H_4)]Br\cdot H_2O$ (**2**)	H_2O	360 (sh), 315 (2600)	diamagnetic
$[LReO(O_2C_7H_6)]Br$ (**3**)	H_2O	667 (50)	diamagnetic
$[LReO(OCH_3)_2](PF_6)$ (**4**)	CH_3CN	680 (39)	diamagnetic
$[LReCl_3](CH_3SO_3)$ (**7**)	5.0 M HCl	1252 (16.4), 1164 (20.3), 1082 (46), 720 (22), 673 (21.3), 620 (5.7)	3.6 μ_B (290 K), 3.4 μ_B (90 K)
$[LReBr_3](CH_3SO_3)$ (**8**)	5.0 M HBr	1320 (28), 1200 (38), 118 (102), 760 (76), 692 (65), 643 (24)	3.6 μ_B (290 K), 3.5 μ_B (90 K)
$[L'_2Re_2Cl_4(\mu\text{-}O)][ZnCl_4]$ (**9**)	0.5 M HCl	690 (sh, 110), 628 (250), 480 (910), 398 (1.3×10^4), 351 (2.4×10^4)	diamagnetic
$[L_2Re_2Cl_2(\mu\text{-}O)_2]I_2\cdot 2H_2O$ (**10**)	1.0 M NaCl	757 (217), 621 (272), 520 (sh), 461 (4500)	diamagnetic
$[L_2Re_2Br_2(\mu\text{-}O)_2]Br_2\cdot 2H_2O$ (**11**)	1.0 M NaBr	768 (230), 625 (245), 477 (5800), 308 (2150), 276 (3550)	diamagnetic
$[L_2Re_2I_2(\mu\text{-}O)_2]I_2\cdot 2H_2O$ (**12**)	1.0 M NaI	776 (290), 630 (300), 497 (6600), 369 (2900), 328 (4100)	diamagnetic
$[L_2Re_2O_2(\mu\text{-}O)_2]I_2$ (**13**)	H_2O	730 (300), 556 (1560)	diamagnetic
$[L_2Re_2Cl_2(\mu\text{-}Cl)(\mu\text{-}OH)]I_2\cdot 2H_2O$ (**15**)	H_2O	940 (250), 660 (sh, 1600), 572 (3000), 310 (sh, 3600)	diamagnetic
$[L_2Re_2Br_2(\mu\text{-}Br)(\mu\text{-}OH)]I_2\cdot 2H_2O$ (**16**)	H_2O	963 (310), 680 (sh, 2400), 603 (3400)	diamagnetic

[a] Molar absorption coefficients for complexes **9–16** are given per dinuclear unit. Measurements at 20 °C.

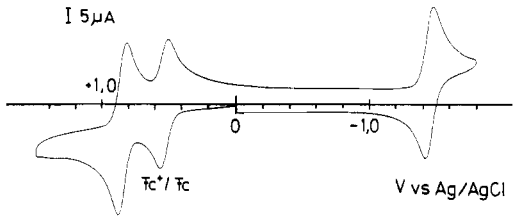

Figure 2. Cyclic voltammogram of $[L'ReO(OCH_3)_2]PF_6$ (**4**) in CH_3CN (0.1 M $[TBA]PF_6$ supporting electrolyte; glassy-carbon working electrode, [**4**] $\approx 10^{-4}$ M; scan rate 0.2 V s^{-1}).

complex $[L'ReO(OCH_3)_2]PF_6$ (**4**), where L' represents 1,4,7-trimethyl-1,4,7-triazacyclononane, is obtained in low yields (≈5%) from the reduction of $[L'ReO_3]^+$ [16] in dry methanol with zinc powder. The PF_6 salt has been isolated as air-stable blue crystals.

Data obtained from the electronic spectra of **1–4** are summarized in Table II. **1**, **3**, and **4** display a single weak absorption maximum in the visible region, which is assigned to a d–d transition. $ReOCl_3(CNCMe_3)_2$,[19] $ReOBr_3(CNCMe_3)_2$,[19] and $ReOCl_3$(triphos))[20] show a similar absorption maximum at 590 nm (ϵ = 44 L mol^{-1} cm^{-1}), 606 nm (80), and 606 nm (21), respectively. In the spectrum of **2**, this band is obscured by a very strong charge-transfer band at 315 nm (2.6×10^3 L mol^{-1} cm^{-1}).

The electrochemistry of **1–4** has been investigated by cyclic voltammetry. The cyclic voltammograms of **1–3** measured in H_2O (0.1 M $LiClO_4$ supporting electrolyte, glassy-carbon working electrode) display an irreversible reduction peak in the potential range +1.5 to −1.6 V vs Ag/AgCl at −1.07, −0.87, and −0.95 V vs NHE at a scan rate of 0.2 V s^{-1}, respectively. The cyclic voltammogram of **4** in acetonitrile (0.1 M $[TBA]PF_6$ supporting electrolyte, glassy-carbon working electrode) displays two reversible one-electron-transfer waves at +0.70 and −1.60 V vs NHE ($E_{1/2}$). Figure 2 shows this cyclic voltammogram at 0.2 V s^{-1} scan rate. We assign these processes to a reversible one-electron oxidation and reduction, respectively, as in eq 1. Attempts to generate the

$$[L'Re^{VI}O(OCH_3)_2]^{2+} \underset{-e^-}{\overset{+e^-}{\rightleftharpoons}} [L'Re^{V}O(OCH_3)_2]^{+} \underset{-e^-}{\overset{+e^-}{\rightleftharpoons}} [L'Re^{IV}O(OCH_3)_2]^{0} \quad (1)$$

oxidized or reduced form of **4** chemically have been unsuccessful to date.

Thermal decomposition of solid **1** affords quantitatively 1 equiv each of ethylene and water and a colorless residue, which was characterized as $[LReO_3]X$[21] (X = Cl, Br, I) according to eq 2.

$$[LRe^{V}O(O_2C_2H_4)]^+ \rightarrow [LRe^{VII}O_3]^+ + C_2H_4 \quad (2)$$

Differential thermal analysis experiments where the iodide monohydrate salt of **1** was heated within 50 min from 20 to 180 °C showed a single exothermic peak at 144 °C. An 8.8% loss of weight was measured, which agrees well with the calculated value of 8.6% assuming the formation of one equiv of ethylene and water, respectively, per formula unit. Mass spectroscopy and gas chromatography showed that ethylene was the only organic reaction product (>98.5%). $Cp^*ReO(O_2C_2H_4)$[22] and $ReOCl(O_2C_2H_4)$(phen)[23] are also thermally decomposed to yield ethylene and Cp^*ReO_3 and ReO_3Cl(phen), respectively. The former reacts at 150 °C whereas the latter requires 220 °C (vacuum).

The bromide (**1**) and iodide salts of $[LRe^{V}O(O_2C_2H_4)]^+$ proved to be a versatile starting material for the syntheses of a variety of mononuclear and dinuclear Re(III) and Re(IV) complexes. Thus reduction of $[LRe^{V}O(O_2C_2H_4)]I\cdot H_2O$ in 1.0 M CH_3SO_3H with an excess of zinc dust at 40 °C affords a clear, green-brown solution. Addition of NaCl and NaBr initiates the immediate precipitation of an orange and red microcrystalline solid material, respectively. Elemental analysis and magnetic properties (see below) showed that the mononuclear species $LReCl_3$ (**5**) and $LReBr_3$ (**6**) had formed in 60% yield. The same products were obtained when $[LRe^{V}O(O_2C_2H_4)]I\cdot H_2O$ was reduced with zinc in 1.0 M hydrochloric or hydrobromic acid. **5** and **6** are nearly insoluble in all common solvents.

In the infrared spectrum of **5**, two Re–Cl stretching frequencies are observed at 310 and 290 cm^{-1}, which is in agreement with C_{3v} symmetry of the N_3ReCl_3 polyhedron (A_1 and E). **6** does not show the corresponding Re–Br vibrations in the experimentally available range 400–180 cm^{-1}.

From magnetic susceptibility data on **5** and **6** in the temperature range 90–298 K, slightly temperature-dependent magnetic moments were calculated: 1.76 μ_B (293 K) and 1.12 μ_B (105 K) for **5** and 1.87 μ_B (293 K) and 1.23 μ_B (105 K) for **6**. Due to strong spin–orbit coupling these magnetic moments are significantly smaller than the spin-only value of 2.83 μ_B for monomeric low-spin Re(III) complexes (d^4). Octahedral Re(III) complexes have magnetic moments in the range 1.5–2.1 μ_B at room temperature.[24]

Heating to 100 °C of a suspension of **5** and **6** in methanesulfonic acid in the presence of air affords a green-brown solution, respectively, from which, upon cooling and addition of diethyl ether, light-green microcrystals of $[LReCl_3](CH_3SO_3)$ (**7**) and $[LReBr_3](CH_3SO_3)$ (**8**) were obtained in 55% yield. **7** and **8** are soluble in water and may be recrystallized as chloride or bromide salts $[LReX_3]X$ (X = Cl, Br) by addition of NaCl or NaBr. In the infrared spectrum of **7**, two Re–Cl stretching frequencies (A_1 and E) are observed at 354 and 337 cm^{-1}, whereas for **8** only the symmetric Re–Br stretching frequency at 230 cm^{-1} has been detected in the available range. The ν(Re–Cl) vibrations of **7**

(19) Bryan, J. C.; Stenkamp, R. E.; Tulip, T. H.; Meyer, J. M. *Inorg. Chem.* **1987**, *26*, 2283.
(20) Davis, R.; Fergusson, J. E. *Inorg. Chim. Acta* **1970**, *4*, 16.
(21) Wieghardt, K.; Pomp, C.; Nuber, B.; Weiss, J. *Inorg. Chem.* **1986**, *25*, 1659.
(22) Herrmann, W. A.; Marz, D.; Herdtweck, E.; Schäfer, A.; Wagner, W.; Kneuper, H.-J. *Angew. Chem., Int. Ed. Engl.* **1987**, *26*, 462.
(23) Pearlstein, R. M.; Davison, A. *Polyhedron* **1988**, *7*, 1981.
(24) Figgis, B. N.; Lewis, J. *Prog. Inorg. Chem.* **1964**, *6*, 37.

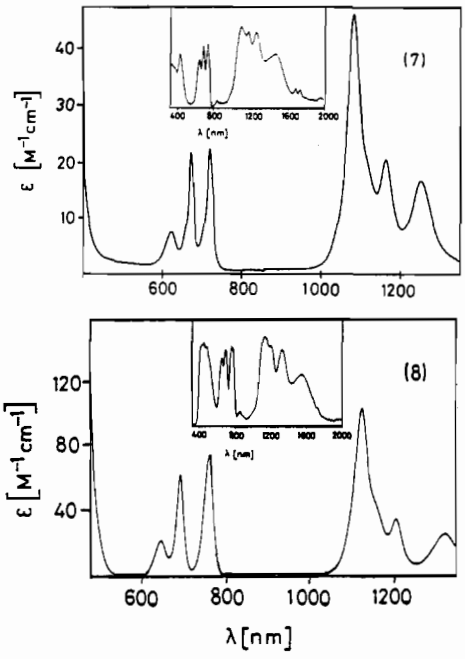

Figure 3. Electronic spectra of $[LReCl_3](CH_3SO_3)$ (**7**) and $[LReBr_3](CH_3SO_3)$ (**8**) in 0.5 M HCl and HBr, respectively, and in the solid state (insets) as reflectance spectra.

shifted to higher wavenumbers as compared to those of **5**. The same effect has been reported for $Re^{IV}Cl_4(PR_3)_2$ and $Re^{III}Cl_3(PR_3)_3$ complexes.[25]

7 and **8** are paramagnetic. Temperature-dependent susceptibility data (90–298 K) could be fitted to the Curie–Weiss law yielding temperature independent magnetic moments of 3.59 μ_B ($\Theta = -13.2$ K) for **7** and 3.61 μ_B ($\Theta = -11.5$ K) for **8**. These values confirm the oxidation state as Re(IV) (d^3) in **7** and **8**.

Figure 3 shows the electronic spectra of **7** and **8** both in solution (400–1350 nm) and in the solid state (reflectance spectra 400–2000 nm). Spectral data are summarized in Table II. The spectra are quite complex and are very similar to those reported for $ReCl_6^{2-}$ and $ReBr_6^{2-}$.[26] We do not assign the absorption maxima in the present work, but this is readily possible in the light of the detailed analysis of the spectra of ReX_6^{2-} species (X = F, Cl, Br, I) in ref 26 if one accounts for the symmetry change from O_h to C_{3v}.

Syntheses of Dinuclear Complexes. Scheme II summarizes the preparative routes to dinuclear rhenium complexes prepared in this work. Reduction of a colorless solution of $[L'ReO_3]I$[16] dissolved in 0.5 M HCl with zinc dust at 60 °C brings about a color change from blue to green and, finally, to deep brown. Addition of $ZnCl_2$ to the cooled solution initiates the precipitation of brown microcrystals of $[L'_2Re^{IV}_2Cl_4(\mu\text{-}O)][ZnCl_4]$ (**9**) in 36% yield. Solutions of **9** in 0.5 M HCl are stable for weeks in the presence of air. Single crystals suitable for an X-ray structure determination were grown from such a solution.

Susceptibility measurements (90–298 K) on the crude product show a weak "residual" paramagnetism (≈0.8 μ_B/dimer), but recrystallized **9** is diamagnetic. This result is important in the light of the discussion of the "residual paramagnetism" reported for $K_4[Re^{IV}_2Cl_{10}(\mu\text{-}O)]\cdot H_2O$[27] and suggests strongly that this material is probably contaminated with a paramagnetic impurity ($[Re_2Cl_{10}(\mu\text{-}O)]^{3-}$ (?)).

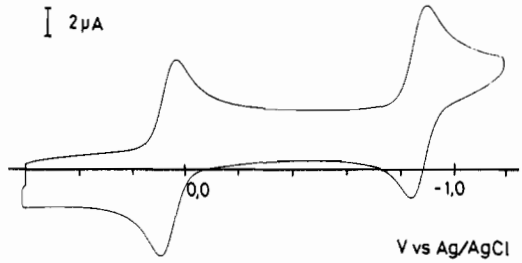

Figure 4. Cyclic voltammogram of $[L'_2Re_2Cl_4(\mu\text{-}O)](ClO_4)_2$ (**9**) in CH_3CN (0.1 M $[TBA]PF_6$ supporting electrolyte, glassy-carbon working electrode; [9] ≈ 10^{-4} M; scan rate 0.2 V s^{-1}).

Scheme II. Syntheses of Dinuclear Complexes

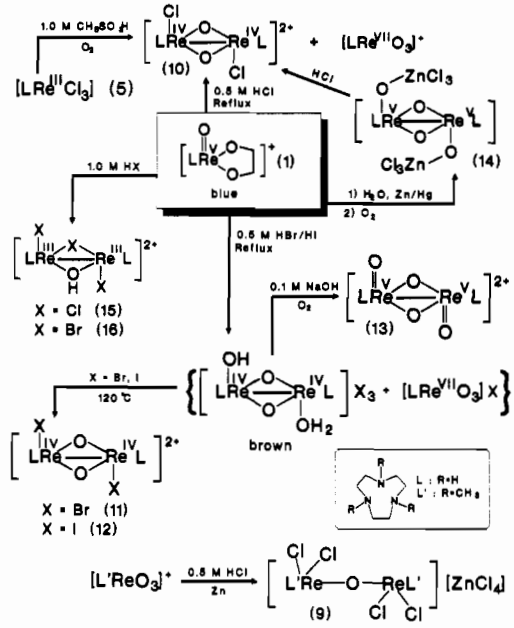

The diperchlorate salt obtained by metathesis of **9** dissolved in nitromethane-d_3 shows a well-resolved ^1H NMR spectrum (80 MHz, 20 °C): a complicated multiplet of the methylene protons of the macrocyclic ligand at δ = 2.9–4.0 and two signals of the methyl protons at δ = 2.4 and 4.7 (ratio 1:2). This is in agreement with the crystal structure determination (see below).

Figure 4 shows the cyclic voltammogram $[L'_2Re_2Cl_4(\mu\text{-}O)](ClO_4)_2$ in acetonitrile (0.1 M $[TBA]PF_6$ supporting electrolyte, glassy-carbon working electrode). In the potential range +1.9 to −1.9 V vs Ag/AgCl, two reversible one-electron-transfer waves are observed at $E_{1/2}$ values of −0.07 and −1.01 V vs NHE. Attempts to oxidize **9** with ferrocenium hexafluorophosphate in CH_3CN failed; only the starting materials were recovered. Controlled-potential electrolysis of **9** at +0.4 V vs Ag/AgCl showed no current. Coulometric measurements at −0.4 and −1.2 V vs Ag/AgCl were unsuccessful due to severe adsorption of **9** at the electrode. We conclude that the electron-transfer processes correspond to two successive one-electron reductions of **9**.

$$[L'_2Re^{IV}_2Cl_4(\mu\text{-}O)]^{2+} + e^- \rightleftharpoons [L'_2Re^{III}Re^{IV}Cl_4(\mu\text{-}O)]^+ + e^- \rightleftharpoons [L'_2Re^{III}_2Cl_4(\mu\text{-}O)]^0 \quad (3)$$

In contrast, $[Re_2(\mu\text{-}O)Cl_{10}]^{4-}$ is readily oxidized to $[Re_2(\mu\text{-}O)Cl_{10}]^{3-}$ by H_2O_2 in dilute HCl.[28] Under the same reaction conditions, **9** is not oxidized.

In the following, we describe a series of disproportionation reactions of **1** that lead to the formation of dinuclear complexes of Re(III), Re(IV), and Re(V). When a solution of **1** in 0.5 M HCl was heated under reflux for a few hours, the original blue color changed to deep brown. Addition of NaI initiates slow

(25) (a) Chatt, J.; Leigh, G. J.; Mingos, D. M. P. *J. Chem. Soc. A* **1969**, 1674. (b) Cariati, F.; Sgamelotti, A.; Morazzi, F.; Valenti, V. *Inorg. Chim. Acta* **1971**, *5*, 531.

(26) (a) Jörgensen, C. K.; Schwochau, K. *Z. Naturforsch.* **1965**, *20A*, 65. (b) Yao, Q.; Maverick, A. W. *Inorg. Chem.* **1988**, *27*, 1670. (c) Kelm, W.; Preetz, W. *Z. Anorg. Allg. Chem.* **1989**, *568*, 106, 117. (d) Pross, L.; Rössler, K.; Schenk, H. J. *J. Inorg. Nucl. Chem.* **1974**, *36*, 317. (e) Eisenstein, J. C. *J. Chem. Phys.* **1961**, *34*, 1628.

(27) (a) Noddack, W.; Noddack, I. *Z. Anorg. Chem.* **1933**, *215*, 129. (b) Jezowska-Trzebiatowska, B. *Trav. Soc. Sci. Lett. Wroclaw, Ser. B* **1953**, *39*, 24. (c) Morrow, J. C. *Acta Crystallogr.* **1960**, *13*, 443. (d) Jezowska-Trzebiatowska, B.; Wajda, S. *Bull. Acad. Pol. Sci., Cl. 3* **1954**, *5*, 2.

(28) Lis, T.; Jezowska-Trzebiatowska, B. *Acta Crystallogr.* **1976**, *B32*, 867.

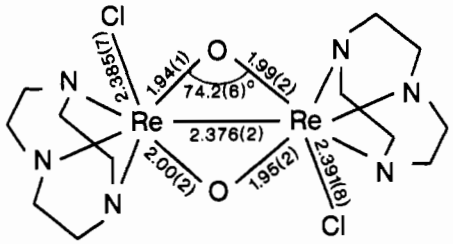

Figure 5. Structure of the dication in crystals of $[L_2Re_2Cl_2(\mu\text{-}O)]I_2 \cdot 2H_2O$ (**10**) with selected bond distances (Å) and angles (deg).[13]

precipitation of black *and* colorless crystals within 2 days. The crystals were separated out manually under a microscope and identified as $[LRe^{VII}O_3]I$ and $[L_2Re^{IV}_2Cl_2(\mu\text{-}O)_2]I_2 \cdot 2H_2O$ (**10**). **10** has been characterized by X-ray crystallography;[13] Figure 5 shows the structure of the dication and gives selected bond distances and angles. The yields of solid **10** did not exceed 30%. Thus in acidic aqueous solution, **1** disproportionates generating a dinuclear Re(IV) and a mononuclear Re(VII) species, (eq 4). The

$$3[LRe^{V}O(O_2C_2H_4)]^+ \xrightarrow{HCl} [L_2Re^{IV}_2Cl_2(\mu\text{-}O)_2]^{2+} + [LRe^{VII}O_3]^+ \quad (4)$$

yield of **10** can be improved to ≈60% when a mixture of **5** in 1.0 M CH_3SO_3H is heated in the presence of air under reflux for 3 h. Under these conditions no $[LReO_3]^+$ formed.

When the above disproportionation reaction of **1** is carried out in 1.0 M HCl, addition of NaI also leads to crystallization of **10** and $[LReO_3]I$ within 2 days at 20 °C. When the filtrate of this solution is stored at 2 °C for a further 2 days, deep blue crystals of $[L_2Re_2Cl_2(\mu\text{-}Cl)(\mu\text{-}OH)]I_2 \cdot 2H_2O$ (**15**) formed in ≈10% yield. The bromo analogue $[L_2Re_2Br_2(\mu\text{-}Br)(\mu\text{-}OH)]Br_2 \cdot 2H_2O$ (**16**) is formed when 1.0 M HBr is used instead of HCl. **15** has been characterized by X-ray crystallography (see below).

Replacing the hydrochloric acid by 0.5 M HBr or 0.5 M HI in the above reaction (eq 4) also induces a disproportionation of **1**. Upon addition of NaBr or NaI, a black-brown solid material was isolated, which in some preparations contained a minor amount of $[LReO_3]Br$ of $[LReO_3]I$. The electronic spectrum of this material is quite similar to that of **10**, but the absorption maxima are shifted to shorter wavelengths. The spectra of the HBr and HI preparations are identical. This effect is in contrast to the expected shift to longer wavelengths if merely the chloro ligands in **10** are substituted by Br^- or I^-. The bromo and iodo analogues of **10**, namely complexes **11** and **12**, have indeed been prepared (see below) and characterized, and their electronic spectra do show the expected shift to longer wavelengths. This indicates that in the brown materials no halogeno ligands are coordinated at the rhenium centers. Elemental analyses indicate a ratio L:Re:X of 1:1:1.5 where X represents Br or I. We propose either of the following structures for these materials.

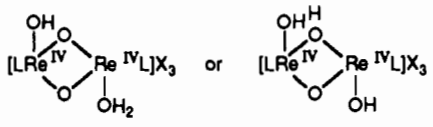

We have not been able to satisfactorily characterize these materials further. The notion of coordinated terminal aqua and/or hydroxo ligands is strongly corroborated by the observation that after the solid materials were heated to 120 °C for a few hours, the complexes $[L_2Re_2Br_2(\mu\text{-}O)_2]Br_2 \cdot 2H_2O$ (**11**) and $[L_2Re_2I_2(\mu\text{-}O)_2]I_2 \cdot 2H_2O$ (**12**) are obtained from aqueous solutions of the so treated materials by addition of NaBr and NaI, respectively. **12** has been characterized by X-ray crystallography (see below). Complexes **10–12** constitute a series of diamagnetic, isoelectronic and isostructural complexes. They are stable in aqueous solution for many hours. No dissociation of halide has been observed.

Figure 6 shows the solution electronic spectra of **10–12**. The most intense absorption in the visible clearly shifts from 461 to 477 nm and, finally, to 497 nm as Cl^- is substituted by Br^- and I^-. This band is observed at 428 nm for the brown-black materials

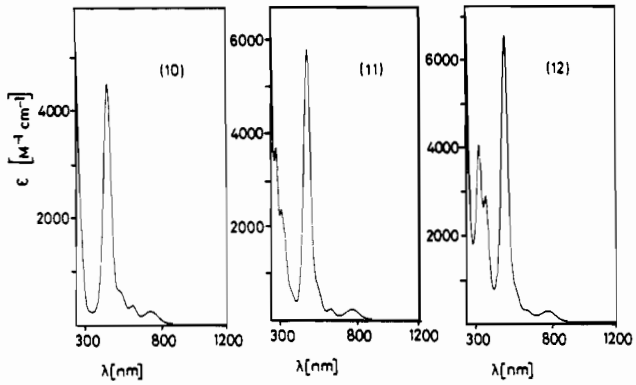

Figure 6. Electronic spectra of **10–12** measured in 1.0 M NaCl, NaBr, and NaI, respectively.

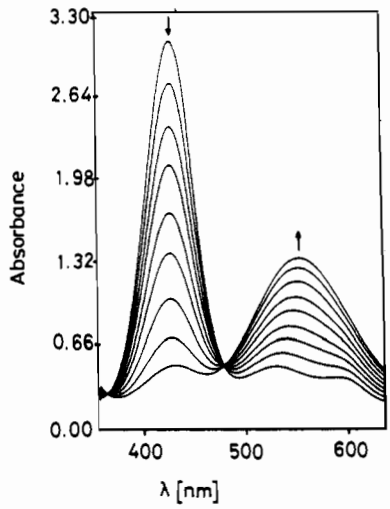

Figure 7. Repetitive scan spectrum of the brown material (≈10^{-3} M) (see text) dissolved in 0.1 M NaOH at 20 °C in the presence of air. Every 3 min a spectrum was recorded.

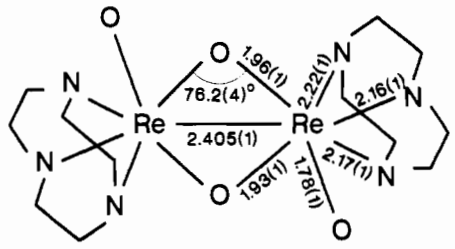

Figure 8. Structure of the dication in crystals of $[L_2Re_2O_2(\mu\text{-}O)_2]I_2$ (**13**) with selected bond distances (Å) and angles (deg).[13]

described above. It is interesting to note that the electronic spectra of $[L_2M^{III}_2Cl_2(\mu\text{-}OH)_2]^{2+}$, where M represents molybdenum or tungsten, are very similar.[29] Since these dinuclear hydroxo-bridged complexes are isoelectronic with the Re(IV) complexes **10–12**, we propose that these bands are due to transitions from occupied metal–metal molecular orbitals ($\sigma^2\pi^2\delta^2$) to unoccupied Re≡Re orbitals ($\pi \rightarrow \pi^*$ transitions).

Alkaline solutions of the above brown precipitates ("$[L_2Re_2(OH)(H_2O)(\mu\text{-}O)_2]X_3$") react readily with oxygen by generating a purple diamagnetic bis(μ-oxo)dirhenium(V) species (**13**). Figure 7 shows a repetitive scan spectrum of this reaction in 0.1 M NaOH ([complex] ≈ 10^{-3} M), which clearly shows two isosbestic points at 368 and 481 nm. The iodide salt *anti*-$[L_2Re_2O_2(\mu\text{-}O)_2]I_2$ has been isolated and characterized by X-ray crystallography.[13] Figure 8 shows the structure and important bond distances and angles of **13**. **13** may also be synthesized in better yields from a deox-

(29) (a) Wieghardt, K.; Hahn, M.; Swiridoff, W.; Weiss, J. *Inorg. Chem.* **1984**, *23*, 94. (b) Schreiber, P. Dissertation, Ruhr-Universität, Bochum FRG, 1989.

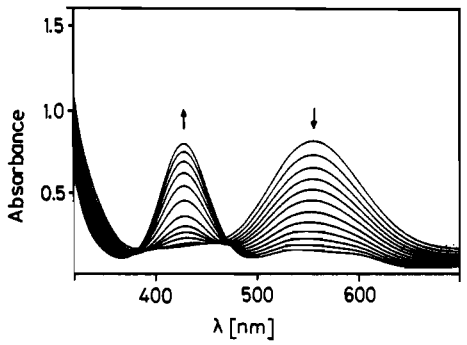

Figure 9. Repetitive scan spectrum of the disproportionation of **13** (5.1 × 10^{-4} M) at 20 °C in 0.1 M methanesulfonic acid. Every 10 min a spectrum was recorded.

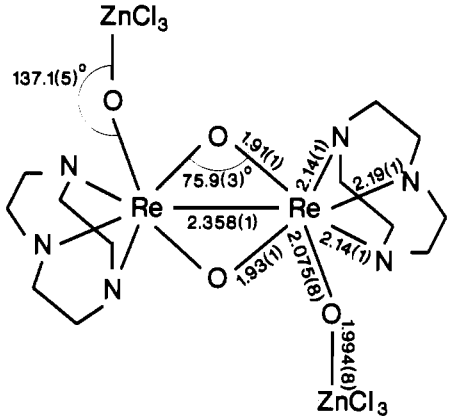

Figure 10. Structure of the neutral species $[L_2Re_2(OZnCl_3)_2(\mu\text{-}O)_2]$ (**14**) with selected bond distances (Å) and angles (deg).[13]

ygenated aqueous solution of **1** to which zinc amalgam was added at 20 °C. After 3 h, the now green-brown solution is separated from the zinc amalgam and exposed to air. Within 24 h the color of the solution changes to purple and addition of NaI initiates the precipitation of **13** in ≈60% yield.

13 disproportionates in 0.1 M methanesulfonic acid under anaerobic conditions to afford the brown putative $[L_2Re^{IV}(OH)(H_2O)(\mu\text{-}O)_2]I_3$ and $[LReO_3]I$. Figure 9 shows a repetitive scan spectrum of this reaction; no isosbestic points are observed in this case. The final spectrum is identical with that described above for the "brown materials".

The terminal Re^{V}=O groups in **13** display nucleophilic properties. Addition of $ZnCl_2$ and NaCl to an aqueous solution of **13** leads to the precipitation of the neutral species $[L_2Re_2(OZnCl_3)_2(\mu\text{-}O)_2]$ (**14**). The crystal structure of **14** has been reported in the preliminary communication of this work.[13] The structure and important bond distances and angles are shown in Figure 10.

Crystal Structure Determinations

(a) Mononuclear Species. Details of the crystal structure determination of $[LReO(O_2C_2H_4)]Br\cdot H_2O$ (**1**) have been reported previously.[13] Figure 1 summarizes the results. The rhenium(V) center is in a pseudooctahedral environment comprised of three facially coordinated nitrogen atoms of the macrocyclic amine, one terminal oxo ligand, and two cis-oriented oxygens of a glycolato ligand. The short terminal Re—O_t bond distance at 1.70 (1) Å agrees well with the average Re—O_t bond length of 41 monooxorhenium(V) complexes at 1.691 Å as analyzed by Mayer[2c,30] and is indicative of a rhenium(V)–oxo triple bond. This bond exerts a pronounced trans influence on the Re—N bond in the trans-position to the Re=O group ($\Delta[(Re—N_{trans}) - (Re—N_{cis})]$ = 0.09 Å). The structure of the organometallic counterpart of **1**, $Cp^*ReO(O_2C_2H_4)$,[22] is very similar. The Re–O distances of the alkoxo–rhenium(V) bonds in **1** are also quite short (average 1.935 Å) and are intermediate between a single and a double bond.

Due to the steric constraints of the ligands L and L′ the N–Re–N bond angles are significantly smaller than the ideal octahedral angle of 90°. This is a common feature of all structures reported in this work and will not be discussed for the following structures. In the absence of disorder effects, the C–C distances of the coordinated amine ligands L and L′ are normal as are the bond angles and will also not be discussed. They are available in the supplementary material.

Crystals of **7** consist of the pseudooctahedral monocation $[LReCl_3]^+$ (Figure 11) and an uncoordinated chloride anion. Table III lists the atom coordinates and Table IV gives bond distances and angles. The structure determination confirms the oxidation state +IV of the rhenium center. The cation possesses crystallographic site symmetry *m* which is not compatible with the (λλλ) or (δδδ) configuration of the three five-membered Re–N–C–C–N chelate rings. Consequently, the C atoms have physically meaningless large anisotropic thermal parameters, and the C–C bond distances appear to be too short. Attempts to refine the structure with a split-atom model for the carbon atoms failed. This feature is frequently encountered in crystal structures of materials containing coordinated macrocycles L and L′.[12a] Although the average Re–Cl distance at 2.310 Å is only slightly shorter than in $[ReCl_6]^{2-}$ at 2.353 (4) Å, it is unclear why the two Re–Cl distances in **7** are significantly different (Re–Cl(2) = 2.331 (3) Å and Re–Cl(3) = 2.289 (4) Å).

(b) Dinuclear Species. Figure 12 shows the structure of the dication in crystals of **9**; atom coordinates are listed in Table V,

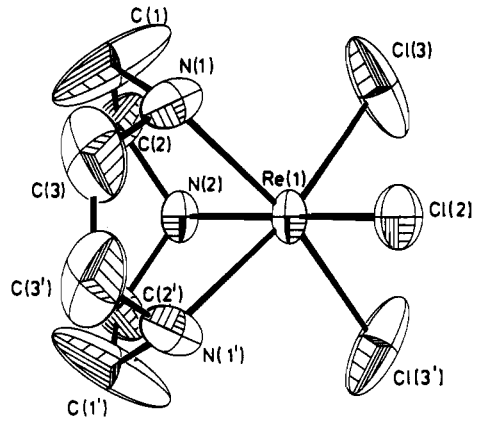

Figure 11. Structure of the cation in $[LReCl_3]Cl$ (**7**) and the atom-labeling scheme.

Table III. Atom Coordinates (×10^4) and Temperature Factors (Å² × 10^3) for **7**

atom	x/a	y/b	z/c	U_{eq}[a]
Re(1)	0	7000 (1)	7165 (1)	40 (1)
Cl(1)	0	1879 (3)	6216 (3)	60 (1)
Cl(2)	0	5867 (2)	8562 (3)	54 (1)
Cl(3)	2157 (6)	6207 (2)	6276 (3)	130 (2)
N(1)	1733 (11)	8008 (6)	7933 (6)	60 (3)
N(2)	0	8289 (6)	6129 (8)	41 (4)
C(1)	2439 (20)	8765 (12)	7169 (11)	188 (10)
C(2)	1599 (14)	8919 (8)	6259 (8)	74 (5)
C(3)	897 (16)	8510 (9)	8834 (9)	110 (7)

[a] Equivalent isotropic *U* defined as one-third of the trace of the orthogonalized U_{ij} tensor.

Table IV. Selected Bond Lengths (Å) and Angles (deg) for **7**

Re(1)–Cl(2)	2.331 (3)	Re(1)–N(1)	2.129 (8)
Re(1)–Cl(3)	2.289 (4)	Re(1)–N(2)	2.139 (9)
Cl(2)–Re(1)–Cl(3)	96.5 (1)	Cl(2)–Re(1)–N(2)	167.8 (3)
Cl(3)–Re(1)–N(1)	92.1 (2)	N(1)–Re(1)–N(2)	79.7 (3)
Cl(3)–Re(1)–N(2)	91.7 (2)	Cl(3)–Re(1)–Cl(3a)	95.3 (2)
N(1)–Re(1)–Cl(3a)	168.8 (2)	Cl(3)–Re(1)–N(1a)	160.8 (2)
Cl(2)–Re(1)–N(1a)	91.0 (2)		
N(1)–Re(1)–N(1a)	79.4 (4)		

(30) Mayer, J. M. *Inorg. Chem.* **1988**, *27*, 3899.

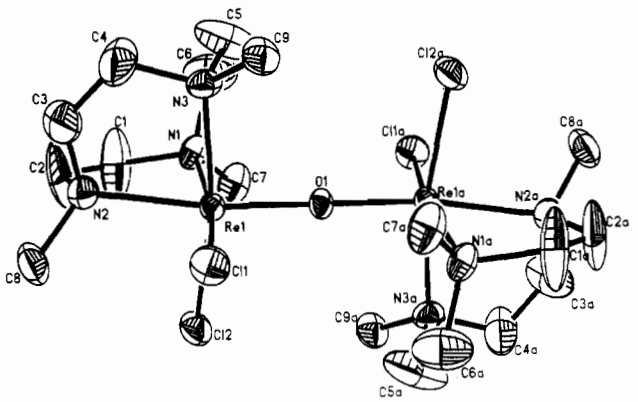

Figure 12. Structure of the dication in crystals of $[L'_2Re_2Cl_4(\mu\text{-}O)][ZnCl_4]$ (**9** and the atom-labeling scheme.

Table V. Atomic Coordinates ($\times 10^4$) and Equivalent Isotropic Displacement Parameters ($Å^2 \times 10^3$) for **9**

atom	x/a	y/b	z/c	U_{eq}[a]
Re(1)	665 (1)	299 (1)	687 (1)	27 (1)
Cl(1)	−504 (3)	1747 (2)	718 (1)	49 (1)
Cl(2)	3057 (3)	946 (2)	428 (1)	51 (1)
O(1)	0	0	0	30 (2)
N(1)	1713 (9)	−1027 (5)	821 (3)	39 (3)
N(2)	1350 (9)	441 (5)	1525 (3)	42 (3)
N(3)	−1265 (9)	−366 (5)	1069 (3)	41 (3)
C(1)	2759 (17)	−935 (10)	1291 (5)	109 (7)
C(2)	2433 (19)	−279 (8)	1661 (5)	105 (6)
C(3)	−135 (18)	350 (10)	1840 (5)	103 (7)
C(4)	−1235 (14)	−193 (11)	1651 (4)	87 (6)
C(5)	−1054 (14)	−1355 (9)	973 (7)	102 (7)
C(6)	463 (16)	−1680 (9)	922 (6)	89 (6)
C(7)	2736 (12)	−1355 (7)	388 (3)	57 (4)
C(8)	2036 (12)	1351 (7)	1679 (4)	59 (4)
C(9)	−2825 (11)	−113 (7)	868 (4)	50 (4)
Zn(1)	2500	2472 (1)	7500	39 (1)
Cl(3)	683 (3)	1577 (2)	7101 (1)	64 (1)
Cl(4)	1105 (3)	3312 (2)	8085 (1)	61 (1)

[a] Equivalent isotropic U defined as one-third of the trace of the orthogonalized U_{ij} tensor.

Table VI. Selected Bond Lengths (Å) and Angles (deg) for **9**

Re(1)–Cl(1)	2.343 (3)	Re(1)–N(1)	2.162 (8)
Re(1)–Cl(2)	2.364 (3)	Re(1)–N(2)	2.207 (7)
Re(1)–O(1)	1.878 (1)	Re(1)–N(3)	2.158 (8)
Re(1)–O(1)–Re(1a)	180.0 (1)	O(1)–Re(1)–N(1)	93.7 (2)
Cl(1)–Re(1)–Cl(2)	91.5 (1)	Cl(1)–Re(1)–N(2)	89.9 (2)
Cl(1)–Re(1)–O(1)	96.2 (1)	Cl(2)–Re(1)–N(2)	89.6 (2)
Cl(2)–Re(1)–O(1)	96.0 (1)	O(1)–Re(1)–N(2)	171.5 (2)
Cl(1)–Re(1)–N(1)	169.0 (2)	N(1)–Re(1)–N(2)	79.7 (3)
Cl(2)–Re(1)–N(1)	92.0 (2)	Cl(1)–Re(1)–N(3)	93.3 (3)
Cl(2)–Re(1)–N(3)	168.2 (2)	O(1)–Re(1)–N(3)	94.1 (2)
N(1)–Re(1)–N(3)	81.4 (3)	N(2)–Re(1)–N(3)	79.7 (3)

and Table VI summarizes selected bond distances and angles. The dinuclear dication lies on a crystallographic inversion center. Each Re(IV) ion is in a pseudooctahedral environment comprised of three nitrogen atoms of the macrocycle L', two chloride ions in the cis position, and an oxygen atom of a μ-oxo bridge. The Re–O–Re angle is at 180°. The two linearly oxo bridged octahedra adopt an eclipsed configuration with the chloride ligands in the anti position relative to each other.

The $Re\text{–}O_{oxo}$ bond distance at 1.878 (1) Å is longer than that in $K_4[Re_2OCl_{10}]\cdot H_2O$[27c] (1.865 (2) Å) but indicates considerable double-bond character. This is also borne out by a significant trans influence of the $Re\text{–}O_{oxo}$ bond on the $Re\text{–}N_{trans}$ bond (Δ-[$(Re\text{–}N_{trans}) - (Re\text{–}N_{cis})$ = 0.047 Å). The average Re–Cl distance at 2.35 Å is typical for Re^{IV}–Cl bonds.

Figure 13 displays the structure of the dication in crystals of **12**, which is isoelectronic and isostructural with that of **10** shown in Figure 5. Atom coordinates of **12** are listed in Table VII, and

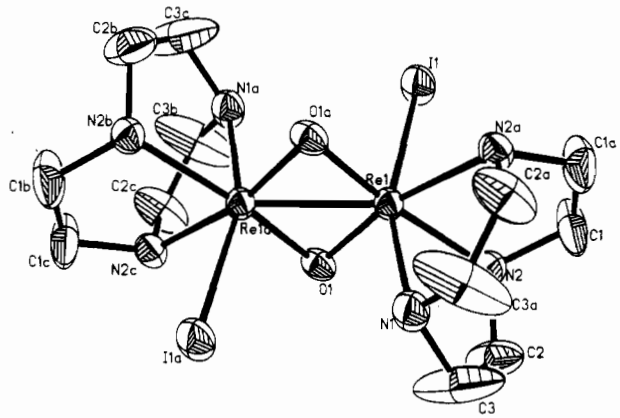

Figure 13. Structure of the dication in crystals of $[L_2Re_2I_2(\mu\text{-}O)_2]I_2\cdot 2H_2O$ (**12**) and the atom-labeling scheme.

Table VII. Atomic Coordinates ($\times 10^4$) and Equivalent Isotropic Displacement Parameters ($Å^2 \times 10^3$) for **12**

atom	x/a	y/b	z/c	U_{eq}
Re(1)	627 (1)	0	670 (1)	27 (1)
I(1)	−866 (1)	0	2142 (1)	45 (1)
I(2)	5555 (1)	0	2202 (1)	45 (1)
O(1)	0	1817 (13)	0	32 (4)
N(1)	2198 (12)	0	−81 (10)	41 (5)
N(2)	1606 (8)	1663 (12)	1526 (6)	34 (3)
C(1)	2090 (13)	897 (18)	2416 (10)	64 (6)
C(2)	2545 (14)	2351 (20)	928 (11)	66 (6)
C(3)	2880 (17)	1492 (23)	133 (14)	113 (9)
O(W)	3836 (16)	0	4396 (17)	142 (13)

Table VIII. Selected Bond Lengths (Å) and Angles (deg) for **12**

Re(1)–I(1)	2.707 (1)	Re(1)–O(1)	1.937 (9)
Re(1)–N(1)	2.144 (15)	Re(1)–N(2)	2.173 (10)
Re(1)–Re(1a)	2.381 (1)	Re(1)–O(1a)	1.937 (9)
Re(1)–N(2a)	2.173 (10)		
I(1)–Re(1)–O(1)	96.1 (1)	I(1)–Re(1)–N(1)	160.2 (4)
O(1)–Re(1)–N(1)	96.1 (2)	I(1)–Re(1)–N(2)	86.9 (2)
O(1)–Re(1)–N(2)	87.7 (3)	N(1)–Re(1)–N(2)	78.0 (4)
I(1)–Re(1)–O(1a)	96.0 (1)	O(1)–Re(1)–O(1a)	104.1 (4)
N(1)–Re(1)–O(1a)	96.2 (2)	N(2)–Re(1)–O(1a)	167.4 (3)
O(1)–Re(1)–N(2a)	167.4 (3)	I(1)–Re(1)–N(2a)	86.8 (2)
N(2)–Re(1)–N(2a)	80.1 (5)	N(1)–Re(1)–N(2a)	78.1 (4)
O(1a)–Re(1)–N(2a)	87.7 (3)		
Re(1)–O(1)–Re(1a)	75.9 (4)		

Table VIII gives selected bond distances and angles. Crystals of **12** consist of the dinuclear species $[L_2Re_2I_2(\mu\text{-}O)_2]^{2+}$, two uncoordinated iodide anions, and two molecules of water of crystallization. Two pseudooctahedral Re(IV) ions are connected by two symmetrical oxo bridges (edge-sharing bioctahedral); the two terminal iodide ligands, one at each Re(IV) center, are in the anti position with respect to each other. The octahedral environment is completed by a tridentate facially coordinated macrocycle L at each Re(IV) ion. The dication possesses crystallographically imposed site symmetry m, which again is not compatible with a ($\lambda\lambda\lambda$) or ($\delta\delta\delta$) configuration of the five-membered Re–N–C–C–N chelate rings, leading to the same crystallographic consequences as described above for **7**. The $Re_2(\mu\text{-}O)_2$ four-membered ring is planar. The Re–Re distance at 2.381 (1) Å is very short and indicative of a strong metal–metal bond ($\sigma^2\pi^2\delta^2$). Consequently, the Re–O–Re angles are acute whereas the O(1)–Re–O(1a) angles are obtuse. It is noted that **10** and **12** do not crystallize in the same space group.

The details of crystal structure determinations of **13** and **14** have been described previously;[13] Figures 8 and 10 show the structures and give important bond distances and angles for **13** and **14**, respectively. In **13** and **14**, two Re(V) ions are connected by two oxo bridges (edge-sharing), respectively; the $Re_2(\mu\text{-}O)_2$ rings are planar. Each Re(V) ion in **13** possesses a terminal oxo group (Re=O = 1.779 (8) Å) both of which are in the anti position with respect to each other. The Re–Re distance at 2.405

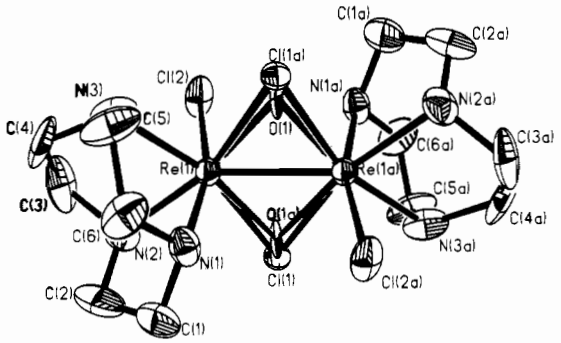

Figure 14. Structure of the dication in crystals of $[L_2Re_2Cl_2(\mu\text{-}Cl)(\mu\text{-}OH)]I_2\cdot 2H_2O$ (**15**) and the atom-labeling scheme.

Table IX. Atom Coordinates ($\times 10^4$) for **15**

atom	x/a	y/b	z/c
Re(1)	5526.7 (6)	5588.8 (7)	3780.8 (5)
I(1)	8542 (1)	9704 (2)	7676 (1)
O(1)	6293 (26)	3390 (33)	4739 (30)
Cl(1)	3227 (11)	7070 (13)	5328 (14)
Cl(2)	3607 (4)	4475 (5)	2573 (3)
N(1)	7445 (13)	6823 (15)	4283 (11)
N(2)	5261 (15)	7796 (15)	2424 (11)
N(3)	7501 (12)	5035 (16)	2059 (13)
C(1)	6888 (20)	8601 (20)	4169 (16)
C(2)	6296 (21)	9060 (20)	2785 (18)
C(3)	5708 (20)	7348 (24)	930 (14)
C(4)	7370 (20)	6313 (25)	791 (13)
C(5)	9130 (18)	4972 (22)	2580 (17)
C(6)	9127 (16)	6416 (22)	3420 (15)
O(W)	11623 (15)	7727 (16)	9530 (13)

(1) Å is short and indicates a metal–metal bond of the order 2 ($\sigma^2\pi^2$). The structure of **14** is very similar. However, the presence of a bound $ZnCl_3^-$ fragment at each of the two terminal oxo ligands leads to a significant increase in the Re–O($ZnCl_3$) distance (2.075 (8) Å) and to a *decrease* in the Re–Re distance (2.358 (1) Å).

Figure 14 shows the structure of the dication in crystals of $[L_2Re^{III}_2Cl_2(\mu\text{-}OH)(\mu\text{-}Cl)]I_2\cdot 2H_2O$ (**15**), Table IX gives the atom coordinates, and Table X summarizes selected bond distances and angles. The dication lies on a crystallographic center of symmetry. As a consequence of this, the dication is disordered. Refinement of the structure proceeded smoothly by using a split-atom model for the bridging O and Cl atoms with an occupancy factor of 0.5, respectively. The quality of the structure determination is not as good as would be desirable; the estimated standard deviations are quite large.

Therefore, it has not been possible to locate the position of the hydrogen atom at the hydroxo bridge. Although the $Re\text{–}O_{hydroxo}$ bond distance at 2.06 (3) Å is quite long and compatible with a bridging hydroxo group, the 3σ value of ≈0.10 Å does not allow a clear distinction from a bridging oxo group. Thus the assignment of an OH^- rather than O^{2-} bridge rests entirely on the fact that the cation in **15** carries a 2+ charge which is counterbalanced by two uncoordinated iodide ions and that **15** is diamagnetic. The alternative formulation $[L_2Re_2Cl_2(\mu\text{-}Cl)(\mu\text{-}O)]I_2\cdot 2H_2O$ would be paramagnetic. The Re–Re distance at 2.528 (1) Å is again indicative of a metal–metal bond. Since **15** is a Re(III) (d^4) dinuclear species with two edge-sharing octahedra, the bond order is formally 2 ($\sigma^2\pi^2\delta^2\delta^{*2}$).

Discussion

The μ-Oxo Species $[L'_2Re^{IV}_2Cl_4(\mu\text{-}O)]ZnCl_4$ (9). This rhenium(IV) species (**9**) is diamagnetic contrasting, in this respect, contradicting reports on "residual paramagnetism" of $K_4[Re_2Cl_{10}(\mu\text{-}O)]\cdot 3H_2O$. The electronic spectrum of **9** is very different from that of $[LRe^{IV}Cl_3]^+$, a simple monomeric octahedral Re(IV) complex, which displays only very weak d–d transitions in the range 300 to 1100 nm ($\epsilon \approx 6$–50 L mol^{-1} cm^{-1}/Re^{IV}). Figure 15 shows the spectrum of **9**, which is dominated by three very intense absorption maxima at 351 (2.4×10^4), 398 (1.3×10^4), and 480 nm (910 L mol^{-1} cm^{-1}). This is a clear indication that strong coupling between the rhenium ions prevails and the system is delocalized. The coupling must occur via the bridging oxide ion. This is corroborated by the crystal structure, which shows that the $Re\text{–}O_{oxo}$ bond is short and exhibits considerable double bond character ($d\pi$–$p\pi$ overlap). The Re^{IV}–O–Re^{IV} unit is linear and the $ReClN_2O$ "equatorial planes" are eclipsed. A qualitative molecular orbital scheme, based on the model by Dunitz and Orgel[31] for $[Cl_5Ru^{IV}\text{–}O\text{–}Ru^{IV}Cl_5]^{4-}$ and modified by Meyer et al.[32] for $[(AA)_2XRu^{III}\text{–}O\text{–}Ru^{III}X(AA)_2]^{2+}$ (AA is 2,2′-bipyridine or 1,10-phenanthroline; X = Cl^-, NO_2^-) is shown in Figure 16. For the labeling of the d orbitals, we chose the Re–O–Re vector as the *z* axis and the two N–Re–Cl vectors define the *x* and *y* axes. Due to the lower symmetry of **9** as compared to $Cl_5Ru\text{–}O\text{–}RuCl_5$ and strong spin–orbit coupling,[33] the degeneracy of the t_{2g} orbitals is lifted. This scheme then immediately explains the magnetic behavior of second- and third-row transition-metal complexes with linear M–O–M units. For Meyer's $Ru^{III}\text{–}O\text{–}Ru^{III}$ complexes 14 electrons (four from occupied p_xp_y orbitals of the O^{2-} bridge and five from each Ru^{III} ion) occupy the molecular orbitals resulting in a diamagnetic ($S = 0$) ground state with $(\pi_1^*)^2$ being the HOMO. The HOMO–LUMO gap ($\pi_1^* - \pi_2^*$) is small and may be directly measured from temperature-dependent susceptibility measurements, which indicate antiferromagnetic coupling ($|2J| = 173$–119 cm^{-1}). Formal removal of two electrons as in $[Cl_5Ru^{IV}\text{–}O\text{–}Ru^{IV}Cl_5]^{4-}$ (12 electrons) yields a singlet ground state with $(\pi_2^n)^2$ being the HOMO. This complex is diamagnetic. Further removal of two electrons leads to complex **9** with 10 electrons (four from p_x, p_y orbitals of the

Table X. Selected Bond Lengths (Å) and Angles (deg) for **15**

Re(1)–O(1)	2.06 (3)	Re(1)–N(1)	2.12 (1)
Re(1)–Cl(1)	2.50 (1)	Re(1)–N(2)	2.17 (1)
Re(1)–Cl(2)	2.410 (4)	Re(1)–N(3)	2.17 (1)
Re(1)–Re(1a)	2.528 (1)	Re(1)–O(1a)	2.07 (2)
Re(1)–Cl(1a)	2.47 (1)		
Cl(1)–Re(1)–O(1)	111.2 (7)	N(2)–Re(1)–Cl(1)	82.2 (4)
Cl(2)–Re(1)–O(1)	92.8 (8)	N(2)–Re(1)–Cl(2)	89.5 (4)
Cl(2)–Re(1)–Cl(1)	92.7 (3)	N(2)–Re(1)–N(1)	78.6 (5)
N(1)–Re(1)–O(1)	96.6 (8)	N(3)–Re(1)–O(1)	86.7 (8)
N(1)–Re(1)–Cl(1)	95.4 (4)	N(3)–Re(1)–Cl(1)	161.9 (4)
N(1)–Re(1)–Cl(2)	164.4 (3)	N(3)–Re(1)–Cl(2)	89.3 (3)
N(2)–Re(1)–O(1)	166.3 (7)	N(3)–Re(1)–N(1)	78.9 (4)
Re(1)–O(1)–Re(1a)	75.7 (8)	N(3)–Re(1)–N(2)	79.8 (4)
Re(1)–Cl(1)–Re(1a)	60.0 (3)		

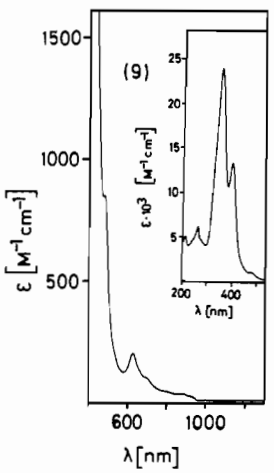

Figure 15. Electronic spectrum of **9** measured in 0.5 M HCl at 20 °C.

(31) Dunitz, J. D.; Orgel, L. E. *J. Chem. Soc. London* **1953**, 2595.
(32) Weaver, T. R.; Meyer, T. J.; Adeyemi, S. A.; Brown, G. M.; Eckberg, R. P.; Hatfield, W. E.; Johnson, E. C.; Murray, R. W.; Untereker, D. *J. Am. Chem. Soc.* **1975**, *97*, 3039.
(33) Hatfield, W. E. In *Theory and Application of Molecular Paramagnetism*; Boudreaux, E. A., Mulay, L. N., Eds.; Wiley: New York, 1976; pp 407–409.

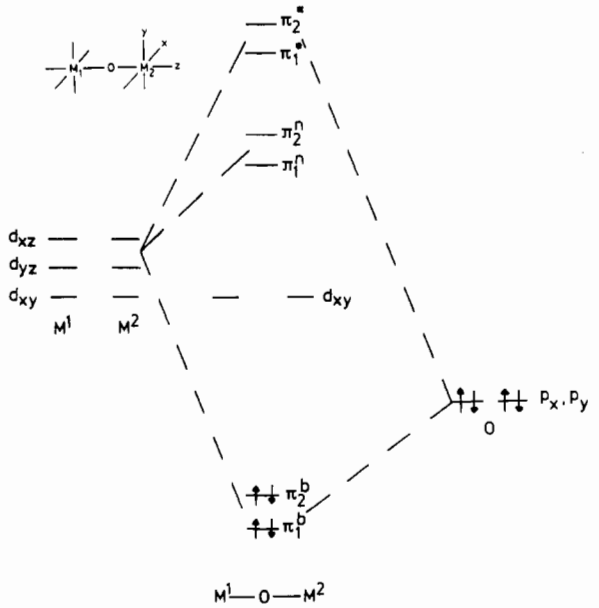

Figure 16. Qualitative molecular orbital scheme for bioctahedral M–O–M complexes.

O^{2-} ion and three from each Re^{IV} ion) which gives $(\pi_1^n)^2$ as the HOMO and an $S = 0$ ground state. Interestingly, the energy gap between π_1^n and π_2^n must be quite large because no paramagnetic contribution from the $(\pi_1^n)^1(\pi_2^n)^1$ state is observed for **9** up to 298 K. The same arguments seem to apply for isoelectronic $[Mo^{III}_2(\mu\text{-}O)(CH_3CN)_{10}](BF_4)_4$,[34] which is also diamagnetic. Following Meyer's analysis of the electronic spectrum of Ru^{III}–O–Ru^{III} species, we suggest that the very intense absorptions at 351 and 398 nm can be assigned to symmetry-allowed $\pi^b \rightarrow \pi^*$ transitions involving delocalized Re^{IV}–O–Re^{IV} levels.

It would be interesting to explore the magnetic properties of the unknown $[Cl_5Mo^{V}\text{–}O\text{–}Mo^{V}Cl_5]^{2-}$ ion or alike complexes because the above molecular orbital scheme predicts an uncoupled paramagnetic behavior. For $[L_2Ti^{III}_2Cl_2(\mu\text{-}O)]^{2+}$, this behavior has been observed,[35] but the delocalized MO model may not be applicable here as is clearly indicated by the observation of very strong ferromagnetic coupling for $[L'_2V^{III}_2(acac)_2(\mu\text{-}O)]^{2+}$ (S = 2 ground state),[36] for which the above scheme predicts a singlet ground state.

The Series *anti*-$[L_2Re^{IV}_2X_2(\mu\text{-}O)_2]^{2+}$ (X = Cl (10), Br (11), I (12)). Table XI summarizes the M–M distances of a series of bioctahedral second- and third-row transition-metal complexes all of which contain a planar $M_2(\mu\text{-}X)_2$ unit (X = OH^- or O^{2-}) and a d^3–d^3 metal ion pair. The M–M distances are in a rather narrow range at 2.33–2.50 Å, and all complexes are diamagnetic. Most importantly, their electronic spectra are very similar. A very intense absorption with molar absorption coefficients >1000 L mol^{-1} cm^{-1} in the visible region (340–520 nm) and approximately three weaker absorption maxima (ϵ < 300 L mol^{-1} cm^{-1}) at longer wavelengths are observed independent of the nature of the respective transition metal (Mo, W, Tc, Re). This is a clear indication that a common metal–metal molecular orbital scheme may be applicable for the electronic configuration for all complexes ($\sigma^2\pi^2\delta^2$ or $\sigma^2\pi^2\delta^{*2}$) giving rise to a formal metal–metal bond order of 1 or 3, respectively. If one assumes the δ and δ^* orbitals to be essentially nonbonding, the M–M bond is probably best described as a double bond.[3,41] It is tempting to assign the intense band in the visible region to a symmetry-allowed $\pi \rightarrow \pi^*$ transition (see below). It is interesting that within the two series of complexes $[L_2W^{III}_2X_2(\mu\text{-}OH)_2]^{2+}$ (X = Cl, Br, I) and $[L_2Re^{IV}_2X_2(\mu\text{-}O)_2]^{2+}$ (X = Cl, Br, I), this band shifts to lower energy with increasing π-donor capability of the terminal ligand X^- ($I^- > Br^- > Cl^-$). It is also tempting to correlate the increasing π-donor capacity of X^- with a concomitant lengthening of the Re–Re bond on going from **10** to **12**, but here the effect is small and may not be significant since both Re–Re distances are the same within an experimental uncertainty of 3 times the estimated standard deviation. This effect is more evident in the following series of dinuclear $Re^{V}_2(\mu\text{-}O)_2$ complexes.

Table XI. Comparison of M–M Bond Distances in Bioctahedral Complexes Containing the $M(\mu\text{-}X)_2M$ Unit (X = O^{2-}, OH^-) and a d^3–d^3 Metal Pair[a]

complex	M–M, Å	λ_{max}, nm[b]	ref
$[L_2Mo^{III}_2Cl_2(\mu\text{-}OH)_2]^{2+}$	2.501 (3)	384 (1.2 × 10^3)	29a
$[L_2W^{III}_2Cl_2(\mu\text{-}OH)_2]^{2+}$		344 (2.3 × 10^3)	40, 29b
$[L_2W^{III}_2Br_2(\mu\text{-}OH)_2]^{2+}$	2.477 (3)	350 (1.7 × 10^3)	29b
$[L_2W^{III}_2I_2(\mu\text{-}OH)_2]^{2+}$		354 (1.6 × 10^3)	29b
$[(H_2edta)_2Tc^{IV}_2(\mu\text{-}O)_2]$	2.331 (1)	495 (2.0 × 10^3)	37
$[(NTA)_2Tc^{IV}_2(\mu\text{-}O)_2]^{2-}$	2.362 (2)	501 (5.0 × 10^3)	38
$[(TCTA)_2Tc^{IV}_2(\mu\text{-}O)_2]^{2-}$		520 (2.4 × 10^3)	39
$[(C_2O_4)_4Re^{IV}_2(\mu\text{-}O)_2]^{4-}$	2.362 (1)		28
$[L_2Re^{IV}_2Cl_2(\mu\text{-}O)_2]^{2+}$ [c]	2.376 (2)	461 (4.5 × 10^3)	13
$[L_2Re^{IV}_2Br_2(\mu\text{-}O)_2]^{2+}$ [d]		477 (5.8 × 10^3)	this work
$[L_2Re^{IV}_2I_2(\mu\text{-}O)_2]^{2+}$ [e]	2.381 (1)	497 (6.6 × 10^3)	this work

[a] Key: L = 1,4,7-triazacyclononane; H_2edta = dihydrogen ethylenediaminetetraacetate(2–). NTA = nitrilotriacetate(3–); TCTA = 1,4,7-triazacyclononanetriyl-1,4,7-triacetate(3–). [b] Most intense transition in the visible region. [c] Cation from **10**. [d] Cation from **11**. [e] Cation from **12**.

Re–Re Bond in Dinuclear Bis(μ-oxo)dirhenium(V) Complexes. Table XII gives a compilation of structures that we will discuss in the following section. It is instructive to first compare the two isomeric forms of dinuclear bioctahedral species, namely *anti*-$[L_2M_2O_2(\mu\text{-}O)_2]^{2+}$ and *syn*-$[L_2M_2O_2(\mu\text{-}O)_2]^{2+}$, where M is Mo(V) and W(V)—a d^1–d^1 metal pair—and corresponding organometallic analogues *anti*-$Cp_2^*M_2O_2(\mu\text{-}O)_2$ and *syn*-$Cp_2^*M_2O_2(\mu\text{-}O)_2$. For the latter species, Bursten and Cayton[43] have shown by Fenske–Hall-type molecular orbital calculations that the syn isomer containing a puckered central $M_2(\mu\text{-}O)_2$ core is more favorable than the anti isomer with a planar $M_2(\mu\text{-}O)_2$ core due to more favorable MO–(μ-O) π-interaction in the folded geometry. It must be kept in mind that these calculations were carried out before the first example of an *anti*-$[Cp_2^*M_2O_2(\mu\text{-}O)_2]$ species with a short M–M bond appeared in the literature. An important observation is that fact that the M–M distance in the bioctahedral complexes is short and invariant of the geometry of the $M_2(\mu\text{-}O)_2$ core. Thus in the anti and syn isomers, the M–M distance is at ≈2.56 Å indicative of a metal–metal single bond (σ^2). This is not the case for the organometallic counterparts where the syn isomer contains a shorter Mo–Mo bond than the anti isomer (Δ = 0.06 Å), which are both slightly longer than in the Werner type bioctahedral complexes by ≈0.06 Å. A further point of interest is the fact that terminal distances in the d^1–d^1 dinuclear complexes are also short and invariant at 1.71 Å. We reiterate the main conclusion from the comparison of d^1–d^1 metal pair complexes: a metal–metal bond is observed in all cases irrespective of the geometry of the $M_2(\mu\text{-}O)_2$ core and irrespective of the $6e^-$ donor ligand, 1,4,7-triazacyclononane or pentamethylcyclopentadienyl(1–).

(34) McGilligan, B. S.; Wright, T. C.; Wilkinson, G.; Montevalli, M.; Hursthouse, M. B. *J. Chem. Soc., Dalton Trans.* **1988**, 1737.
(35) Bodner, A.; Della Vedova, S. P. C.; Wieghardt, K.; Nuber, B.; Weiss, J. *J. Chem. Soc., Chem. Commun.* **1990**, 1042.
(36) (a) Knopp, P.; Wieghardt, K.; Nuber, B.; Weiss, J.; Sheldrick, W. S. *Inorg. Chem.* **1990**, *29*, 363. (b) An S = 2 ground state may also prevail in $[(bpy)_4V_2Cl_2(\mu\text{-}O)]^{2+}$: Brand, S. G.; Edelstein, N.; Hawkins, C. J.; Shalimoff, G.; Snow, M. R.; Tiekink, E. R. T. *Inorg. Chem.* **1990**, *29*, 434.
(37) Bürgi, H. B.; Anderegg, G.; Blåuenstein, P. *Inorg. Chem.* **1981**, *20*, 3829.
(38) Anderegg, G.; Müller, E.; Zollinger, K.; Bürgi, H. B. *Helv. Chim. Acta* **1983**, *66*, 1593.
(39) Linder, K. E.; Dewan, J. C.; Davison, A. *Inorg. Chem.* **1989**, *28*, 3820.
(40) Chaudhuri, P.; Wieghardt, K.; Gebert, W.; Jibril, I.; Huttner, G. *Z. Anorg. Chem.* **1985**, *521*, 23.
(41) Cotton, F. A.; Wilkinson, G. *Advanced Inorganic Chemistry*, 5th ed.; Wiley: New York, 1988; pp 1085–1086.
(42) Hoffmann, P.; Mattes, R. *Inorg. Chem.* **1989**, *28*, 2092.
(43) Bursten, B. E.; Cayton, R. H. *Inorg. Chem.* **1989**, *28*, 2846.

Table XII. Comparison of M–M and M–$O_{terminal}$ Distances in Dinuclear Bis(μ-oxo)dimetal(V) Complexes

complex[a]	M–M, Å	M–$O_{terminal}$, Å	geometry[b]	ref
anti-$[L_2Mo_2O_2(\mu\text{-}O)_2]^{2+}$	2.561 (1)	1.696 (5)	pl	4a
syn-$[L_2Mo_2O_2(\mu\text{-}O)_2]^{2+}$	2.555 (1)	1.695 (6)	pu	4a
anti-$[L_2W_2O_2(\mu\text{-}O)_2]^{2+}$	2.568 (1)	1.73 (1)	pl	4d
syn-$[L_2W_2O_2(\mu\text{-}O)_2]^{2+}$	2.565 (1)	1.72 (1)	pu	4d
syn-$[L^1{}_2Mo_2O_2(\mu\text{-}O)_2]^{2+}$	2.549 (1)	1.680 (5)	pu	42
anti-$[Cp_2{}^*Mo_2O_2(\mu\text{-}O)_2]$	2.647 (3)	1.72 (1)	pl	5b
syn-$[Cp_2{}^*Mo_2O_2(\mu\text{-}O)_2]$	2.587 (1)	1.692 (3)	pu	5a
anti-$[L_2Re_2O_2(\mu\text{-}O)_2]^{2+}$	2.405 (1)	1.779 (8)	pl	13
anti-$[L_2Re_2(OZnCl_3)_2(\mu\text{-}O)_2]$	2.358 (1)	2.075 (8)	pl	13
anti-$Cp_2{}^*Re_2O_2(\mu\text{-}O)_2$	3.142	1.689 (3)	pl	10
syn-$[Cp_2{}^*Re_2Cl_2O(\mu\text{-}O)_2]$	2.691 (1)	1.681 (3)	pu	10
syn-$[Cp_2{}^*Re_2Cl_4(\mu\text{-}O)_2]$	2.72		pu	10
syn-$[Cp_2{}^*Re_2O(ORe^{VII}O_3)_2(\mu\text{-}O)_2]$	2.651 (1)	1.72 (1)	pu	*c*

[a] The prefixes anti and syn designate the positions of the M=O groups or Cp*-ligands relative to each other. L = 1,4,7-triazacyclononane; Cp* = pentamethylcyclopentadienyl(1–); L^1 = 1-thia-4,7-diazacyclononane. [b] Geometry of the $M_2(\mu\text{-}O)_2$ four-membered ring: pl = planar; pu = puckered. [c] Herrmann, W. A.; Serrano, R.; Küsthardt, U.; Ziegler, M. L.; Guggolz, E.; Zahn, T. *Angew. Chem., Int. Ed. Engl.* **1984**, *23*, 515.

The situation changes dramatically when similar complexes containing d^2–d^2 metal pair complexes are compared. *anti*-$[L_2Re^V{}_2O_2(\mu\text{-}O)_2]^{2+}$ contains a short Re–Re bond at 2.405 Å, which is in agreement with the expected shortening on going from d^1–d^1 complexes to d^2–d^2 species with a M–M double bond ($\sigma^2\pi^2$). On the other hand, Herrmann's organometallic counterpart $Cp_2{}^*Re_2O_2(\mu\text{-}O)_2$ obviously does not contain a direct Re–Re bonding interaction. Both complexes contain a planar $Re_2(\mu\text{-}O)_2$ core, and the Re–O_{bridge} distances are identical within experimental error at 1.96 ± 0.02 Å. A significant difference between the two $O_2Re_2(\mu\text{-}O)_2$ cores exists—not withstanding the different Re–Re distances: The Re=O_t bond is shorter in the organometallic species than in the bioctahedral complex by 0.09 Å. This difference is real as is borne out by the differing ν(Re=O) stretching frequencies, which are observed at 935 cm^{-1} for $[Cp_2{}^*Re_2O_2(\mu\text{-}O)_2]$ and at 818 and 794 cm^{-1} for $[L_2Re_2O_2(\mu\text{-}O)_2]^{2+}$. In rhenium(V) monooxo complexes, this mode is observed in the region 845–985 cm^{-1}.[44]

We propose that this difference is the main cause for the structural diversity of the two compounds. In Herrmann's compound the two terminal oxo groups are much stronger π-donors where the p orbitals interact strongly with the antibonding σ^* and π^* metal–metal orbitals, thereby weakening this bond to an extent that the two d electrons are stabilized in a metal-centered orbital. In $[L_2Re_2O_2(\mu\text{-}O)_2]^{2+}$, this interaction is much weaker and metal–metal molecular orbitals are stabilized. A consequence of this hypothesis is the prediction that weakening of the Re=O_t bond—or their complete replacement by less strong π-donor ligands—will lead to dinuclear Re(V) complexes with direct metal–metal bonding.

The chemistry of these d^2–d^2 complexes unravelled to date seems to support this view. The terminal Re=O groups in $[L_2Re_2O_2(\mu\text{-}O)_2]^{2+}$ display nucleophilic character as is shown by the synthesis of $[L_2Re_2(OZnCl_3)_2(\mu\text{-}O)_2]$. Coordination of the $ZnCl_3^-$ fragment to the Re=O group leads to a substantial lengthening of the Re—O bond by 0.295 Å but, concomitantly, to a *shortening* of the Re–Re bond by 0.047 Å. In contrast, Herrmann's compound reacts with the electrophile H^+ by protonation at the oxo bridges forming $[Cp^*{}_2Re_2O_2(\mu\text{-}OH)_2]^{2+}$—the Re=O groups are not protonated.[45] Finally, replacement of one or two terminal oxo groups in $Cp^*{}_2Re_2O_2(\mu\text{-}O)_2$ leads to organometallic complexes (Table XII), all of which contain Re–Re bonds at 2.65–2.72 Å, because the π-donor ability is now reduced.

The effect of π-donor capacity of terminal ligands on the Re–Re metal–metal bond length has previously been discussed by Cotton et al. for the pair of structurally very similar complexes $[Re^{III}{}_2Cl_5(OC_2H_5)(Ph_2PCH_2PPh_2)_2]$ (Re–Re = 2.667 (1) Å) and $[Re^{III}{}_2Cl_6(Ph_2PCH_2PPh_2)_2]$ (Re–Re = 2.616 (1) Å).[46]

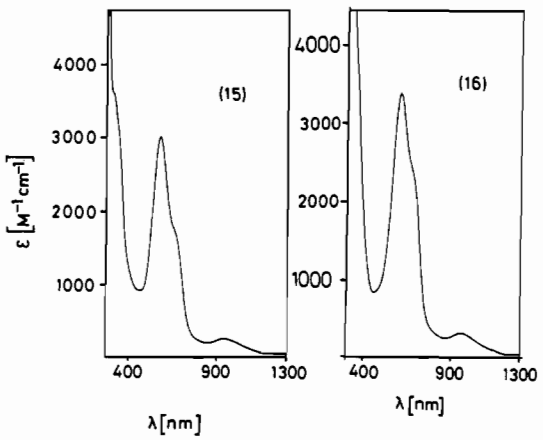

Figure 17. Electronic spectra of **15** and **16** measured in H_2O at 20 °C.

It is noteworthy that the same interpretation may apply for the observation that in the solid-state materials $Nd_4Re^V{}_2O_{11}$[7] and $La_6Re_4O_{18}$,[8] both of which contain bioctahedral $O_8Re^V{}_2(\mu\text{-}O)_2$ building blocks, extremely short Re–Re distances at 2.42 and 2.46 Å, respectively, are observed. In contrast, in $PbRe^V{}_2O_6$,[47] which also contains $\{O_8Re_2(\mu\text{-}O)_2\}$ units, the Re–Re distance is at 3.102 (1) Å, indicating the *absence* of an M–M bond. Fuess et al.[47] have ascribed the abnormal behavior of $PbRe_2O_6$ to packing effects. A comparison of the four "terminal" Re–O bond lengths at each Re^V center in such an $\{O_8Re_2(\mu\text{-}O)_2\}$ unit reveals that the average Re–O_t distance in $PbRe_2O_6$ is 1.888 Å whereas in $Nd_4Re_2O_{11}$ this distance is 2.027 Å and in $La_6Re_4O_{18}$ it is 1.935 Å (here the Re–O_b distances are also quite long, 2.003 Å). Thus we propose that the differing Re–Re distances in these materials have an electronic origin. In $Pb_2Re_2O_6$, the rhenium(V) ions experience stronger π-donation from the terminal oxygen ligands than in $Nd_4Re_2O_{11}$ and $La_6Re_4O_{18}$, and consequently, the former has no Re–Re bond whereas the latter exhibits a strong bonding Re–Re interaction. The π-donor capacity of the terminal oxo ligands is of course tuned by the electrophilicity of Nd^{3+} and La^{3+}, which are strong Lewis acids, and Pb^{2+}, which is a nucleophile rather than an electrophile. A further interesting aspect of this work concerns the electronic spectra of $[L_2M_2X_2(\mu\text{-}O)_2]^{n+}$ species on changing the electronic configuration from d^1–d^1 to d^2–d^2 and to d^3–d^3 yielding single, double and—possibly—triple metal–metal bonds. The very intense absorption maximum in the visible region discussed in the previous section for the d^3–d^3 complexes is also present in $[L_2Re_2O_2(\mu\text{-}O)_2]^+$—a d^2–d^2 species with a $\sigma^2\pi^2$ Re–Re double bond—at 556 nm ($\epsilon = 1.6 \times 10^3$ L mol^{-1} cm^{-1}), but this band is not observed for the d^1–d^1 complexes with a σ^2 single M–M bond. This supports the assignment to a π–π^* transition. The

(44) (a) Blower, P. J.; Dilworth, J. R.; Hutchinson, J. P.; Nicholson, T.; Zubieta, J. *J. Chem. Soc., Dalton Trans.* **1986**, 1339. (b) Jezowska-Trzebiatowska, B.; Hanuza, J.; Baluka, M. *Spectrochim. Acta* **1971**, *27A*, 1753.

(45) Herrmann, W. A. *J. Organomet. Chem.* **1986**, *300*, 111 and references therein.

(46) Barder, T. J.; Cotton, F. A.; Lewis, D.; Schwotzer, W.; Tetrick, S. M.; Walton, R. A. *J. Am. Chem. Soc.* **1984**, *106*, 2882.

(47) Wentzell, I.; Fuess, H.; Bats, J. W.; Cheetham, A. K. *Z. Anorg. Allg. Chem.* **1985**, *528*, 48.

absence of any such intense transitions in the spectrum $[LReO(O_2C_2H_4)]^+$ excludes the presence of intense Re=O ligand-to-metal charge-transfer bands in the visible region.

Properties of $[L_2Re^{III}_2X_2(\mu\text{-}X)(\mu\text{-}OH)]^{2+}$ Complexes (X = Cl, Br). **15** and **16** are the first examples of dirhenium(III) (d^4) complexes containing a planar $\{Re^{III}_2(\mu\text{-}X)(\mu\text{-}OH)\}^{4+}$ core. The Re-Re distance at 2.528 (1) Å and the observed diamagnetism are indicative of a metal-metal bond of the order 2 ($\sigma^2\pi^2\delta^2\delta^{*2}$). The electronic spectra of **15** and **16** both exhibit again the strong π-π^* transition in the visible region (Figure 17). Cotton et al. have reported the structures of two similar compounds: the mixed valence paramagnetic species $[Re^{III}Re^{IV}Cl_2(C_2H_5CO_2)_2(PPh_3)_2(\mu\text{-}O)(\mu\text{-}Cl)]$[48] (Re-Re 2.514 (1) Å) and the diamagnetic rhenium(IV) complex $[Re^{IV}_2Cl_4(PPh_3)_2(C_2H_5CO_2)(\mu\text{-}O)(\mu\text{-}Cl)]$[49] (Re-Re = 2.522 (1) Å). Both Re-Re bonds are shorter than in **15** in agreement with the removal of one and two electrons, respectively, from an antibonding δ^* molecular orbital.

Acknowledgment. We thank the Fonds der Chemischen Industrie for financial support and the Degussa (Hanau, FRG) for a generous loan of rhenium metal.

Supplementary Material Available: A list of crystallographic data, intensity measurements, and details of refinements (Table S1) and tables of anisotropic displacement parameters, H atom coordinates, bond lengths, and bond angles for **7**, **9**, **12**, and **15** (10 pages); listings of observed and calculated structure factors for these four structures (42 pages). Ordering information is given on any current masthead page.

(48) Cotton, F. A.; Eiss, R.; Foxman, B. M. *Inorg. Chem.* **1969**, *8*, 950.

(49) Cotton, F. A.; Foxman, B. M. *Inorg. Chem.* **1968**, *7*, 1784.

Contribution from the Department of Chemistry, Harvard University, Cambridge, Massachusetts 02138, and Francis Bitter National Magnet Laboratory, Massachusetts Institute of Technology, Cambridge, Massachusetts 02139

Comprehensive Iron-Selenium-Thiolate Cluster Chemistry

Shi-Bao Yu,[†] G. C. Papaefthymiou,[‡] and R. H. Holm*,[†]

Received February 12, 1991

Reconstitution of apoferredoxins and other proteins with iron salts and selenide has resulted in the incorporation of Fe_nSe_n clusters in proteins whose native clusters are Fe_nS_n (n = 2, 4). These nonnative clusters have proven useful in interpreting certain electronic features of native clusters, and tend to occur in "high-spin" forms ($S \geq {}^1/_2$). These observations have prompted investigation of a comprehensive set of Fe-Se-SR clusters. Reaction of $(Et_4N)_2[Fe(SEt)_4]$ with 1 equiv of elemental Se in acetonitrile affords $(Et_4N)_2[Fe_2Se_2(SEt)_4]$ (**1**, 55%). Ligand substitution of **1** with 4 equiv of PhSH gives $(Et_4N)_2[Fe_2Se_2(SPh)_4]$ (**2**, 72%), which crystallizes in the orthorhombic space group $P22_12_1$ with a = 8.819 (2) Å, b = 15.813 (3) Å, c = 15.996 (3) Å, and Z = 2. The cluster contains a planar $Fe_2(\mu_2\text{-}Se)_2$ core with Fe-Fe = 2.795 (2) Å. Reaction of $(Et_4N)_2[Fe(SEt)_4]$ with 1.4 equiv of elemental Se in acetone gives $(Et_4N)_3[Fe_3Se_4(SEt)_4]$ (**3**, 67%), which with PhSH is converted to $(Et_4N)_3[Fe_3Se_4(SPh)_4]$ (**4**, 66%). Compound **4** crystallizes in the monoclinic space group $C2/c$ with a = 27.591 (5) Å, b = 11.124 (2) Å, c = 20.961 (3) Å, β = 118.18 (1)°, and Z = 4. The $Fe_3(\mu_2\text{-}Se)_4$ core is linear with Fe-Fe = 2.781 (1) Å and has an $S = {}^5/_2$ ground state. The reaction system $FeCl_3$/Se/4NaSEt in ethanol assembles $(Et_4N)_2[Fe_4Se_4(SEt)_4]$ (**5**, 66%), which was obtained in orthorhombic space group $Pcab$ with a = 17.395 (2) Å, b = 18.387 (3) Å, c = 25.007 (4) Å, and Z = 8. The $[Fe_4(\mu_3\text{-}Se)_4]^{2+}$ core has the familiar cubane stereochemistry with an compressed tetragonal distortion from cubic symmetry. Reduction of **3** with Zn in acetonitrile or **5** with sodium acenaphthylenide in THF/acetonitrile gives $(Et_4N)_3[Fe_4Se_4(SEt)_4]$ (**6**, 56-68%), which crystallizes in monoclinic space group $P2_1/n$ with a = 11.639 (4) Å, b = 36.774 (7) Å, c = 11.875 (2) Å, β = 106.79 (2)°, and Z = 4. The $[Fe_4(\mu_3\text{-}Se)_4]^{1+}$ core has an $S = {}^3/_2$ ground state and virtually the same compressed tetragonal distortion as **5**. The reaction system $FeCl_3$/Na_2Se_2/3NaSEt assembles $(Et_4N)_4[Fe_6Se_9(SEt)_2]$ (**7**, 68%); the $[Fe_6Se_9]^{2-}$ core structure has been previously established in another cluster. Thus, stable Fe-Se clusters of nuclearities 2, 3, 4, and 6 that are structurally and electronically analogous to Fe-S clusters can be prepared. When compared, analogous Fe-Se clusters exhibit red-shifted absorption spectra, less negative redox potentials, larger ^{1}H isotropic shifts, larger paramagnetism, and essentially identical ^{57}Fe isomer shifts. Of all properties, isotropic shifts most readily distinguish Fe-S and Fe-Se clusters of the same nuclearity. Comparison of the structures of $[Fe_4Q_4]^{2+}$ structures (Q = S, Se) provides strong evidence that a compressed tetragonal geometry is the intrinsically preferred structure of this oxidation state. In contrast, a range of structures is found for $[Fe_4Q_4]^+$ clusters that includes compressed and elongated distortions. The existence of compressed and elongated $[Fe_4Se_4]^+$ cores in different compounds with the same ground state ($S = {}^3/_2$) forms part of the evidence that for $[Fe_4Q_4]^+$ clusters there is no relation between core distortion and ground state. While synthetic and protein-bound $[Fe_4Se_4]^+$ clusters with the $S = {}^3/_2$ ground state have been realized, no synthetic clusters with the $S = {}^7/_2$ state claimed in reconstituted clostridial proteins have been detected. The set of analogous Fe-Q clusters (Q = S, Se) also extends to the basket clusters $Fe_6S_6(PR_3)_4X_2$; only the prismane clusters with the $[Fe_6(\mu_3\text{-}Se)_6]^{4+,3+}$ cores have not yet been prepared.

Introduction

It is now well established that at least some ferredoxin apoproteins can be reconstituted with $Fe^{II,III}$ and a selenide source to afford holoproteins containing the binuclear $Fe_2(\mu_2\text{-}Se)_2$ or cubane-type $Fe_4(\mu_3\text{-}Se)_4$ clusters. Thus, apoproteins of bacterial,[1] adrenal,[2] and plant ferredoxins[3,4] have been reconstituted to proteins with Fe_2Se_2 clusters. One Fe_4Se_4 cluster has been placed in the *Chromatium* high-potential protein[5,6] and in beef heart aconitase,[7] and two such clusters have been incorporated in clostridial ferredoxin.[8] Certain of the reconstitutions are among the earliest chemical experiments done with apo- and holoferredoxins[1-3] and are analogues or modifications of the classic work of Rabinowitz and co-workers,[9] who first reconstituted clostridial apoferredoxin with Fe^{II} and sulfide. Contemporary work

[†] Harvard University.
[‡] MIT.

(1) (a) Tsibris, J. C. M.; Namtvedt, M. J.; Gunsalus, I. C. *Biochem. Biophys. Res. Commun.* **1968**, *30*, 323. (b) Orme-Johnson, W. H.; Hansen, R. E.; Beinert, H.; Tsibris, J. C. M.; Bartholomaus, R. C.; Gunsalus, I. C. *Proc. Natl. Acad. Sci. U.S.A.* **1968**, *60*, 368.
(2) Mukai, K.; Huang, J. J.; Kimura, T. *Biochem. Biophys. Res. Commun.* **1973**, *50*, 105; *Biochim. Biophys. Acta* **1974**, *336*, 427.
(3) Fee, J. A.; Palmer, G. *Biochim. Biophys. Acta* **1971**, *245*, 175, 196.
(4) Meyer, J.; Moulis, J.-M.; Lutz, M. *Biochim. Biophys. Acta* **1986**, *871*, 243.
(5) Moulis, J.-M.; Lutz, M.; Gaillard, J.; Noodleman, L. *Biochemistry* **1988**, *27*, 8712.
(6) Sola, M.; Cowan, J. A; Gray, H. B. *J. Am. Chem. Soc.* **1989**, *111*, 6627.
(7) Surerus, K. K.; Kennedy, M. C.; Beinert, H.; Münck, E. *Proc. Natl. Acad. Sci. U.S.A.* **1989**, *86*, 9846.
(8) (a) Meyer, J.; Moulis, J.-M. *Biochem. Biophys. Res. Commun.* **1981**, *103*, 667. (b) Moulis, J.-M.; Meyer, J. *Biochemistry* **1982**, *21*, 4762.

0020-1669/91/1330-3476$02.50/0